UNIVERSITY OF MINNESOTA
ST. ANTHONY FALLS HYDRAULIC LABORATORY
LORENZ G. STRAUB, Director

Technical Paper No. 36, Series B

Ventilated Cavities on Submerged Three-Dimensional Hydrofoils

by

F. R. SCHIEBE and J. M. WETZEL

Prepared for
OFFICE OF NAVAL RESEARCH
Department of the Navy
Washington, D. C.
Project NR 062-192, Contract Nonr 710(04)

December 1961
Minneapolis, Minnesota

UNIVERSITY OF MINNESOTA
ST. ANTHONY FALLS HYDRAULIC LABORATORY
LORENZ G. STRAUB, Director

Technical Paper No. 36, Series B

Ventilated Cavities on Submerged Three-Dimensional Hydrofoils

by

F. R. SCHIEBE and J. M. WETZEL

Prepared for
OFFICE OF NAVAL RESEARCH
Department of the Navy
Washington, D. C.
Project NR 062-192, Contract Nonr 710(04)

December 1961
Minneapolis, Minnesota

PREFACE

In many cases, it has been found desirable in the study of cavity flows to vary the cavity pressure by injecting a gas into the cavity and thereby controlling the cavitation number. To effectively control the cavitation number, the basic mechanism of air entrainment must be found and related to the quantity of gas injected into the cavity. The studies described in this report were directed to obtain information on this problem for hydrofoils of finite span submerged below a free surface. The studies were conducted in the St. Anthony Falls Hydraulic Laboratory.

The investigation was conducted during the period November 30, 1960, to February 28, 1962. The work was sponsored by the Office of Naval Research under Project NR 062-192, Contract Nonr 710(04).

Many members of the Laboratory staff were involved in various details of the program. C. E. Bowers critically reviewed the report. The bulk of the experimental data was taken by W. Parmenter and Z. Tarapore. K. Yalamanchili was primarily responsible for data reduction and F. Thomas for carriage operations. Dr. Song supplied the data from the free-jet water tunnel. Preparation of the manuscript for printing was carried out by Marveen Minish, Marjorie Olson, and Carol Takyi under the general supervision of Loyal Johnson.

ABSTRACT

Experimental studies have been made to determine the air-entrainment rates of ventilated cavities for hydrofoils of finite span submerged below a free surface. The study was divided naturally into two parts; reentrant-jet cavities and pulsating or trailing-vortex cavities. A correlation parameter has been derived to permit determination of the air-entrainment rates for cavities in the reentrant-jet regime assuming that all the air is lost from the cavity through the reentrant jet. As air was also lost through the tip vortices, some dependence was noted with aspect ratio. Air entrainment was a function of velocity for a given cavitation number and ambient pressure. Cavity instability or pulsation was observed at high air-injection rates for thin cavities. Trailing vortices were observed for thick cavities at the higher injection rates. The frequency of the pulsations tended to increase as the foil approached the free surface.

Measurements of lift and drag forces indicated little effect of the free surface for submergence ratios of 1 to 3 chords. Data extrapolated to $\sigma = 0$ agreed favorably with theory by Johnson, and data at the higher σ correlated with theory by Cumberbatch.

C O N T E N T S

LIST OF ILLUSTRATIONS

VENTILATED CAVITIES ON SUBMERGED THREE-DIMENSIONAL HYDROFOILS

I. INTRODUCTION

With the higher speeds attained with hydrofoil craft, it is apparent that the supporting foils will be operating under fully cavitating conditions for considerable periods. It is thus necessary to utilize profiles that retain good force characteristics in the supercavitating-flow regime. Under natural cavitating conditions, the degree of cavitation will be primarily influenced by the ambient pressure as related to the submergence of the foil and by the velocity of the craft. The force characteristics for the profile vary with the cavitation number. It may be desirable for certain regions of operation to exercise some additional control of the cavitation number. This can be done by injecting a gas into the cavity, resulting in an increase in the cavity pressure and a decrease in cavitation number. Thus, by gas injection it is possible to create cavities at relatively low velocities. It is also possible in some cases to create a cavity in a wake region where normally a cavity could not be present for the given ambient conditions. The cavity developed by this process is referred to as a ventilated cavity. It has been previously found that the force and cavity characteristics are essentially the same in both cases for natural and ventilated cavities, provided the cavitation numbers are the same. As the type of gas injected into the cavity should have no effect on the cavity, air may be chosen for convenience.

To determine the economical feasibility of utilizing ventilated cavities, it is necessary to have knowledge as to the quantity of gas required to achieve ventilation to a specified degree. Such information can be obtained in laboratory tests at relatively low velocities. The presence of a free surface may be expected to have some influence on the ventilation process. The investigations described in this report were initiated to obtain information of this type. The objectives of the current program were to experimentally determine the effects of the free surface on air-entrainment rates, force characteristics, cavity length, and cavity stability for hydrofoils of finite span and compare the results with theory whenever possible. Earlier work reported under this contract is given in References [1]* and [2].

---

*Numbers in brackets refer to the List of References at end of paper.

It is necessary to know the basic mechanism by which the air leaves the cavity to satisfactorily predict the air requirements. A description is given of various possible mechanisms of air entrainment and a correlation parameter for reentrant-jet cavities is discussed.

II. GENERAL CONSIDERATIONS

It is convenient to discuss the relationship between the air requirements and the cavitation number by referring to two rather distinct regions. The first region, in which the air demand is proportional to the cavitation number, is called the reentrant-jet region. The second region, in which the air demand is essentially independent of the cavitation number, has been associated with a pulsating cavity as well as formation of trailing vortices at the rear of the cavity and is called the pulsating trailing-vortex region for the purpose of this report.

The reentrant-jet region is probably the region of most practical interest since increasing the air supply beyond certain limits will not further reduce the cavitation number and will also produce the possible disadvantages of excessive air requirements and cavity pulsation. It is therefore desirable to establish these limits or conditions under which operation in the reentrant-jet region is possible.

Air is being released in a reentrant-jet cavity on a foil of finite span in three rather distinct ways: (1) through the tip vortices, (2) diffusion through the cavity walls, and (3) mixing in the reentrant jet itself.

Cuthbert [3] has attempted to analyze the reentrant-jet region for two-dimensional cavities in which tip vortices are not present. He concluded that the quantity of air lost by diffusion through the cavity walls was small compared to the air lost at the rear of the cavity. Photographs and observations of ventilated bodies in the towing tank and the free-jet water tunnel at the St. Anthony Falls Hydraulic Laboratory tend to give strength to this conclusion. It was then assumed that the phenomenon governing the entrainment was either the mixing in the region of the reentrant jet or the method by which the air was transported to the rear of the cavity. A parameter was proposed to describe the former, but was dismissed when considerable scatter was found in the data plotted with this correlating parameter. Attention was then directed to the method of air transport in the cavity and the experimental data

were plotted utilizing parameters derived from this approach.

In the current program, observation of the cavity flows created a rather strong impression that the mixing in the reentrant jet was the governing factor. With this in mind, a slight modification has been made in the parameter as utilized by Cuthbert. If it is assumed that all of the air supplied to the cavity is being entrained in the reentrant jet, and that the entrained air moves at the same velocity as the jet, then the equation of continuity can be written

$$W = cw_a A^* V_j = cP_a A^* V_j / RT \tag{1}$$

where W = air-flow rate into the cavity in lb per sec,
c = concentration of voids by volume in the reentrant jet,
P_a = partial pressure of the air in the cavity in lbs per sq ft,
R = gas constant for air = 53.3 ft lbs per lb per degree Rankine,
T = cavity temperature in degrees Rankine,
A^* = area of reentrant jet in sq ft,
V_j = velocity of reentrant jet in ft per sec, and
w_a = specific weight of the air in the cavity in lbs per cu ft.

By using energy principles and assuming no losses, the well-known relationship between the free-stream velocity V_o, cavity-wall velocity V_c, and V_j can be written

$$V_c = V_j = V_o \sqrt{1 + \sigma} \tag{2}$$

where σ = cavitation number based on cavity pressure, $\dfrac{P_o - P_c}{1/2\rho V_o^2}$.

The assumption of no energy loss in the reentrant jet is somewhat weak. There is, of course, some amount of energy loss which can not be calculated at present. However, in this analysis a functional correlation parameter is being sought rather than a detailed description of the entrainment mechanism. It will be shown later that the concentration of voids in the reentrant jet calculated by means of this analysis is closely verified by direct measurement.

The area of the reentrant jet, A^*, can be determined from the momentum equation in terms of the drag on the body

$$D = \rho_j V_j A^* (V_o + V_j) = C_D \, 1/2 A \rho V_o^2 \tag{3}$$

where D = drag on body in lbs,
ρ_j = density of air-water mixture in reentrant jet in slugs per cu ft,
ρ = water density in slugs per cu ft,
A = area of body between separation points in sq ft, and
C_D = drag coefficient.

The density of the air-water mixture, ρ_j, in the reentrant jet can be expressed in the following form

$$\rho_j = c\rho_a + \rho(1 - c) \tag{4}$$

Since the density of the air, ρ_a, is small compared to the density of the water, ρ, it is reasonable to assume that

$$\rho(1 - c) >> c\rho_a$$

Combining Eqs. (2), (3), and (4), the area of the reentrant jet is

$$A^* = \frac{C_D A}{2(1 - c)} \frac{1}{[1 + \sigma + \sqrt{1 + \sigma}]} \tag{5}$$

This area reduces to the area given in Birkoff [4] when $c = 0$. Now combining Eqs. (1), (2), and (5), the air-flow rate is

$$W = \frac{c P_a V_o A C_D}{2(1 - c)\,[1 + \sqrt{1 + \sigma}]\,RT} \tag{6}$$

Perhaps the greatest difficulty in using this expression is in determining the value of the concentration, c. It was thus attempted to evaluate c experimentally through measurements of the drag coefficient C_D, σ, and W, and use it as a correlation parameter.

Rewriting Eq. (6)

$$c = \frac{2W(1 + \sqrt{1 + \sigma})RT}{P_a V_o AK} \tag{7}$$

where

$$K = C_D + \frac{2W(1 + \sqrt{1 + \sigma})RT}{P_a V_o A}$$

This development can be carried further by setting the total cavity pressure equal to the sum of the partial pressures of the air and water vapor in the cavity.

$$P_c = P_a + P_v \tag{8}$$

The cavity pressure may also be expressed in terms of the velocity and cavitation number.

$$P_c = P_o - \frac{\sigma\rho}{2} V_o^2 \tag{9}$$

Combining Eqs. (6), (8), and (9), the air-flow rate is

$$W = \frac{cC_D A}{2RT(1 - c)\,[1 + \sqrt{1 + \sigma}]} \left[(P_o - P_v)V_o - \frac{\sigma\rho}{2} V_o^3 \right] \tag{10}$$

or

$$W = \frac{c}{1 - c} \frac{\rho V_o^3 AC_D \sigma_v [1 - \frac{\sigma}{\sigma_v}]}{213T[1 + \sqrt{1 + \sigma}]} \tag{11}$$

where σ_v = cavitation number based on water vapor pressure, or

$$\frac{P_o - P_v}{1/2\ \rho V_o^2}$$

Thus, to hold a constant σ, it is apparent that the air demand will increase with velocity at low velocities, reach a maximum, and then fall off to zero

as the velocity becomes sufficient to maintain a natural cavity at the desired cavitation number. That is, $W = 0$ when

$$(P_o - P_v)V_o = \frac{\sigma\rho}{2} V_o^3$$

or

$$\sigma = \frac{P_o - P_v}{1/2\rho V_o^2} = \sigma_v$$

In order to determine the velocity where the air demand is maximum, the differential of Eq. (10) with respect to velocity is

$$\frac{\partial W}{\partial V} = \frac{cC_D A}{2RT(1 - c)\ [1 + \sqrt{1 + \sigma}]} \left[(P_o - P_v) - \frac{3\sigma\rho}{2} V_o^2\right] = 0$$

or

$$V_{o_{W\ max}} = \sqrt{\frac{2(P_o - P_v)}{3\sigma\rho}} \tag{12}$$

Therefore, the maximum air demand for a desired cavitation number is

$$W_{max} = \frac{cC_D A(P_o - P_v)}{3RT(1 - c)\ [1 + \sqrt{1 + \sigma}]} \sqrt{\frac{2(P_o - P_v)}{3\sigma\rho}} \tag{13}$$

at $V_{o_{W\ max}}$

If Eq. (6) is made dimensionless,

$$\frac{W}{w_a V_o A C_D} = \frac{c}{2(1 - c)\ [1 + \sqrt{1 + \sigma}]} \tag{14}$$

where $w_a = \frac{P_a}{RT}$.

The left side of Eq. (14) was essentially the parameter utilized in the analysis by Cuthbert, who rejected it after the experimental data available to him exhibited considerable scatter when plotted in this manner. The

air-flow data used by Cuthbert were obtained from Reference [5]. No drag data were presented in that report. It thus appears that the drag data must have been secured from another source and may have caused some of the objectionable scatter.

The concentration, c, has been plotted as a function of σ in section IV for a wide range of foil geometries and flow conditions and was found to be essentially a linear function of σ. This will be discussed more fully in that section. If the concentration factor is determined by experiment, and if C_D can be calculated for a given foil operating under specified conditions, then the air requirements for any given σ and velocity can be determined from Eq. (10) or (11).

It is also interesting to note that since W varies directly with C_D, a foil selected for optimum performance will also require the least amount of air to achieve the given cavitation number. It may also be expected that as the air supply to the cavity is increased, a point may be reached at which another mechanism of air release from the cavity would be required. In this case, it appears that the cavity would begin to pulsate and/or display vortex tubes at the rear of the cavity.

Song [6] has developed a theory of pulsating cavities by extending resonant bubble theory to the case of a resonating two-dimensional cylinder. Results imply that pulsation will occur with slender cavities and only in the region of a free surface and would not be found in an incompressible fluid of infinite extent. In the free-jet tunnel, the flow was vertical and two free surfaces were present. Hence, a gravity field normal to the cavity was absent and ambient conditions were ideal for pulsating cavities.

The existence of vortex tubes was found in earlier investigations made at the California Institute of Technology [7] to determine the air entrainment behind a circular disk submerged below a free surface. It was found that as the air-flow rate was increased, the cavitation number decreased until a minimum was reached. From this point, the cavitation number could no longer be reduced even for very considerable increases in the air-flow rate. It was found that two rather distinct flow regions existed: a reentrant-jet region and a trailing-vortex region. The reentrant jet was observed for the relatively low air-flow rates and correspondingly high cavitation number. In the region where the air-flow rate had little effect on σ, the reentrant jet

disappeared and twin trailing vortices were observed at the rear of the cavity. The rather sudden increase in air demand was then associated with the trailing vortices, which were assumed to act as pipes carrying the air from the cavity.

Cox and Clayden [8] have developed a theory based on aerodynamic conditions which determined the size of the vortex tubes. It was assumed that since the cavity pressure remains essentially constant, the velocities on the upper and lower side of the cavity must differ because of the hydrostatic pressure difference on the cavity walls. This gave rise to a circulation which permitted an approximation to the size of the vortex tubes. The analysis was complete up to the determination of an experimental constant related to the friction factor of these tubes, which actually served to make the data fit the theoretical curve. Campbell and Hilborne [9] have extended the theoretical and experimental work of Cox and Clayden, also using circular disks placed normal to the flow. The experimental studies were conducted in a rotating arm facility. Of particular interest were effects of the boundaries, both the tank bottom and the free surface, on air requirements. They also found that for the lower air-flow rates and consequently higher cavitation numbers a reentrant jet exists in the cavity. As the air flow was increased and the cavitation number decreased, the reentrant jet disappeared and trailing vortices were found at the rear of the cavity which acted as pipes to carry away air from the cavity. This would partially account for the high air-flow requirements in this region.

Campbell and Hilborne also assumed that the difference in hydrostatic pressure on the upper and lower side of the cavity created a circulation which formed twin trailing vortices at the rear of the cavity. A theoretical analysis was made with certain assumptions as to the maximum cavity thickness and length for a circular disk based on previous experiments by other investigators. The resulting expression was written in terms of a nondimensional entrainment coefficient

$$C_{Qd} = \frac{Q}{U_o d^2} = \frac{\pi}{15.8\, F^4 \sigma^4} \qquad (15)$$

where Q = volume of gas at cavity pressure entrained per unit time,

U_o = velocity of disk,

d = disk diameter,

F = $U_o / \sqrt{gd}$ Froude number based on disk diameter, and

σ = cavitation number based on cavity pressure.

This parameter provides a reasonable prediction for air entrainment which agrees broadly with the experimental results. It also indicated why the data of C. I. T. were found to correlate roughly with the product of σ and F. An investigation was also made of the effect of Froude number based on disk diameter on the air demand, and a correlation between air demand and the product of σ and Froude number was found. Tests conducted in fluids with various surface tensions indicated that surface tension had little or no effect on the air quantity for a given σ.

III. EXPERIMENTAL APPARATUS AND PROCEDURE

A. Towing Facility

The experimental studies described in this report were conducted in a towing tank 9 ft wide, 6 ft deep, and about 200 ft long. A self-propelled carriage was used to obtain speeds up to 18 fps for these tests, the top speed being determined in this case by the time required to obtain a steady cavity and the available length of channel for a test run. The water depth for all tests was maintained at 4.5 ft.

B. Hydrofoils

The foils used for this series of tests were flat plate and modified Tulin-Burkart sections of dimensions as listed in the following table. Only rectangular planforms were utilized.

Chord - in.	Span - in.	Aspect Ratio	Type
2	5	2.5	Flat Plate Profile
3	7.5	2.5	Flat Plate Profile
4	10	2.5	Flat Plate Profile
3	12	4	Flat Plate Profile
3	18	6	Flat Plate Profile
2.5	7.5	3	0.3 x 3° Tulin Profile

The cross section of the majority of the flat plate hydrofoils used was a 6-degree wedge with a hand-sharpened leading edge. In a few cases, a

foil with a profile of an 11.3-degree isosceles triangle with a 2-in. base was utilized.

Air was introduced into the cavity by ports at the base of the strut with a supplementary supply to the leading edge in most cases. The photograph of Fig. 1 shows a typical example of a hydrofoil constructed in this manner. A few tests were run introducing air to the cavity at the tips of the hydrofoil and other tests were run with air introduction at various points along the sides of a sting on a sting-mounted foil. A discussion and observations concerning the various methods of air introduction to the cavity are included in section IV.

The strut in all cases was an NACA 0012 section with a 2-in. chord.

C. Instrumentation

The cavity pressure was measured with a 1 psid Statham pressure transducer mounted directly on the strut above the water surface. A hypodermic tube running the length of the strut connected the transducer with a chamber machined into the suction face of the foil and located aft of the midchord. A membrane of very thin diaphragm rubber was loosely placed over the chamber. The entire system then was filled with water. This type of pressure-measurement system permitted a continuous record of the cavity pressure during the test run, although it was not suitable for measuring pressure fluctuations.

A 2-1/2 psid Statham miniature pressure transducer was mounted directly on a 4-in. by 10-in. foil with its diaphragm exposed to the interior of the cavity. This arrangement was used in pilot studies of a limited nature to detect transient and unsteady cavity behavior such as cavity pulsations.

The air-flow rate was measured with an orifice meter placed in the supply line. Two air tanks on the carriage were used as the air supply. An essentially constant reservoir pressure was maintained by means of a pressure reducer placed in the line between the air tanks and the orifice meter. Pressures and temperatures were recorded to permit determination of the air-flow rate.

The foil strut was attached to a device that permitted adjustment of the angle of attack within 1/4 degree and a dynamometer for measuring lift and drag forces for the various cavity conditions. The unit was attached to a towing strut with which the submergence could be varied. The dynamometer

was a two-component strain-gage type in which the lift and drag could be recorded independently, simultaneously, and continuously during the test.

The force and pressure signals were recorded on a Sanborn four-channel recorder mounted on the carriage. A record of the instantaneous carriage speed was also obtained. This permitted a direct determination of the length of test run, which was extremely useful in evaluating the significance of transient effects of the cavity associated with the acceleration of the carriage.

D. Procedure

The foil was set at a given angle of attack and submergence. The angle of attack was measured from the chord line and the submergence was measured from the water surface to the leading edge of the foil in all cases, as shown in Fig. 2. The chord, C, was taken as the distance from leading to trailing edge. The Reynolds number based on chord for the plate varied from 1×10^5 to 6×10^5 at an essentially constant water temperature of 17 C. Submergences of 2, 2.5, 3, 4, 6, and 9 in. were selected, although all submergences were not used for each profile. Runs were first made for a particular angle of attack and submergence with no air admitted to the foil to determine the extent of natural ventilation, if any. For all tests reported, no cavitation or ventilation of any type was observed until the metered air was supplied in the region of the foil. Also, only cases where supercavitation occurred (cavity covering the entire chord or more of the foil) are reported.

Before each run, the air-flow rate was adjusted to a predetermined value. After the carriage acceleration period and a full cavity across the span was formed, the flow rate was again checked. The cavity pressure and forces were continuously recorded with the Sanborn recorder. As the test run was rather short at the higher velocities, it was not readily convenient to obtain information as to hysteresis effects created by reducing the air flow to the cavity after a full cavity had once been established. Photographs of the cavity were then taken with a 200 μ sec electronic flash for a number of conditions and were used to determine cavity lengths. A reference mark was made on the Sanborn record at the instant the photo was taken. A stroboscopic light was used to visually determine the extent of vibration as evidenced by the formation of waves on the surface of the cavity.

IV. DISCUSSION OF RESULTS

A. Methods Used to Ventilate Cavities

Various methods were utilized to inject air into the cavity. Original tests were conducted by venting air into the cavity by ports at the base of the strut. The air was directed outward along the upper surface of the hydrofoil. Difficulty was experienced in forming a cavity on foils operating at angles of attack of less than 12 degrees and particularly for those foils with chords larger than 2 inches. In view of this difficulty, tests were made introducing the air to the cavity at various locations on the hydrofoils.

In one series of tests, the air was introduced directly at the tips of the hydrofoil. To prevent the jets of air from excessively disrupting the flow in the region of the tips, small deflectors were provided that directed the air jets downstream essentially perpendicular to the foil span. This method of air injection was still unsatisfactory in its ability to form a cavity early in the test run. The upper surface of the cavity on foils vented in this manner was observed to be much clearer than cavities on foils with base-of-strut venting, particularly for the higher discharges, indicating less interaction between the air flow and the cavity itself. The air requirement for foils vented in this manner also seems to be very slightly reduced.

In later tests and in most of the tests reported in this paper, air was vented into the cavity through ports on the base of the strut, as in the original tests, and a supplementary air supply was provided to the leading edge to force ventilation at small angles of attack. This was accomplished by running a separate air-supply line down the strut and embedding it in the foil to a distance of a quarter of an inch from the leading edge. An excessive amount of air introduced in this region disturbed the upper wall of the cavity and was considered an undesirable condition. A needle valve in this line permitted satisfactory regulation. A typical hydrofoil utilizing vents of this type has been shown in the photograph of Fig. 1. This method of air injection proved satisfactory, in that a cavity could be formed almost immediately at the beginning of a test run.

Tests were also run on a hydrofoil mounted on a sting with ports located in the sides of the sting. The air was directed along the surface of the hydrofoil in the same manner as in the case of the strut-mounted foil. However, this sting was provided with several vents, all of which could be

plugged. This provided a convenient method of investigating the effect of introducing air at various distances relative to the hydrofoil. It was found that as long as the supplementary supply to the leading edge was operative, the position of the vents on the sting was completely arbitrary as long as they were located forward of the trailing edge of the foil. Vents located aft of the trailing edge of the foil would not form a cavity even with a relatively large amount of air supplied to the leading edge.

Another method was tried to form cavities at the lower angles of attack. This method was based on the hysteresis properties of ventilated cavities. A device was constructed that permitted a sudden decrease in the angle of attack. In operation, the foil was set at an angle for which a cavity could easily be formed during the acceleration period. After a cavity was developed, the angle of attack was decreased to a lower value. It was found that the cavity would remain on the foil for the lower angles of attack. However, essentially the same lower limit of attack angle was obtained by utilizing the more convenient method of introducing air to the leading edge. Therefore, the hysteresis method was not employed in further tests.

It was thus determined that the vents should be located in such a position that the stream of air will not be directed against, or in any way disrupt, the cavity walls. If the cavity wall is disrupted, more air will be required to maintain the desired cavity. In accordance with this, the momentum of the entering airstream should be kept low. This could possibly be accomplished by employing a greater number of ports. If tip vortices are present and small cavitation numbers are contemplated, a portion of the air could be vented through the tips. For conditions under which forced ventilation is necessary, an air supply to the leading edge or at the normal cavity separation point is important to insure formation of the cavity. A relatively small supply of air to this region should suffice. A large quantity of air in this region is highly undesirable as the cavity wall would become turbulent and more air would be required to maintain a cavity of given characteristics.

B. Mechanisms of Air Entrainment

It was observed that in the case of ventilated bodies traveling normal to the gravitational field and in the vicinity of a free surface there were essentially five different mechanisms of entrainment.

In section II, it was indicated that the major mechanisms of air release from the cavity were entrainment of air in the reentrant jet, loss by a pulsation phenomenon, and loss by trailing vortices formed by the gravitational field. Inasmuch as these phenomena were discussed in section II, they will not be discussed here except to point out some effects of aspect ratio on reentrant-jet cavities. At aspect ratios of 4 and 6, the reentrant jet normally did not occur alone but was accompanied by one or more sets of small trailing vortices.

The two remaining methods of air release are through the tip vortices and through turbulent diffusion at the cavity wall.

Since all hydrofoils tested in this program were of rectangular planform, tip vortices were present in every case. The exact role of these tip vortices in the entrainment process is not known at the present time. For foils at low angles of attack and without the supplementary air supply to the leading edge, the air introduced along the upper surface of the foil was swept downstream and a cavity was not formed immediately. The air was diffused as bubbles into the region of the tip vortices, producing hollow vortex cores far downstream of the hydrofoil. These inflated tubes then slowly moved closer to the foil until they became attached to the tips of the hydrofoil. At the time of attachment, the cavity formed across the entire span. This behavior was particularly noted for relatively low air-supply rates. Thus, it seems a possibility that for certain conditions at high σ, lost air is actually being "fed back" to the cavity by means of the tip vortices. However, at low σ, i.e., high cavity pressures, it seems unrealistic for the air to return to the cavity and some air is probably being lost through the tip vortices. The exact role of the tip vortices should be determined by future research.

Small amounts of air pass through the cavity wall by turbulent diffusion. General observations of cavity flows in the free-jet water tunnel have shown a boundary-layer effect on the cavity attached to the trailing edge of the foil. The cavity changed from a laminar, transparent surface to a turbulent, white, opaque surface a short distance (less than a half inch) aft of the trailing edge. In this white region, observations with stroboscopic lights showed small amounts of air being entrained and carried away from the cavity wall by the stream. However, the cavity wall which sprang from the sharp leading edge remained clear until disrupted by the reentrant jet at the

rear of the cavity. This boundary-layer effect was observed on the cavity wall attached to the trailing edge of the foil in the towing tank also. High air-flow rates into the cavity also created considerable turbulence of the cavity wall.

C. Air-Entrainment Rates

As previously mentioned, the relationship between the quantity of air required to achieve a specified cavitation number can be separated into two rather well-defined regions: a reentrant-jet region and a pulsating-cavity or trailing-vortex region. The value of σ at which the division between these regions occurs was found to depend on submergence, velocity, chord, and aspect ratio. A typical plot of air requirements for a flat plate profile at a given angle of attack is shown in Fig. 3. It will be noted that the division occurs at about $\sigma = 0.1$. As the foil nears the free surface, the reentrant jet persists for smaller σ. Note that a minimum σ exists for each submergence.

It has been found that the angle of attack could be eliminated as a variable by incorporating it into the denominator of the air-flow parameter as $\sin \alpha$. Typical results are shown in Fig. 4 for two angles of attack. Velocity had a considerable effect on air-flow requirements as seen in Fig. 5. The curves presented are lines faired through experimental data, such as obtained from Fig. 4. To avoid confusion, the data have not been shown on this plot. In the reentrant-jet region, air requirements to maintain a constant σ tended to increase with increasing velocity at those low velocities. The critical σ, or the value of σ at which the reentrant jet disappears, was also influenced by velocity. As the velocity increases, the critical σ was slightly lower, with the result that a lower σ could be obtained for the same air-flow rate.

In an attempt to find the correlation parameter that would eliminate the effect of velocity on air requirements in the reentrant-jet region, the development previously summarized in section II was carried out. As a result, the concentration, c, described by Eq. (7) was used as a parameter for plotting the experimental data. This parameter is valid only in the reentrant-jet region; therefore the experimental data used were restricted to that region. The shape of the body should have little effect on the parameter. A brief series of tests was conducted in which the concentration of air in the reentrant

jet was measured directly with an electronic concentration meter available at the Laboratory. This meter is described in Reference [10]. The measured values agreed well with the calculated values as shown in Fig. 6 for a submergence of one chord. It will be shown later that submergence has no effect on the concentration factor. This agreement was encouraging, and thus a wider range of variables was considered in more extensive tests. The concentration factor was found to be useful in correlating data taken at different submergences, velocities, angles of attack, chords, and cambers. The data form essentially a straight line relating the concentration and σ, as can be seen in Fig. 7. Different aspect ratios produce slightly different slopes of the line (Fig. 7f). An empirical equation relating concentration, cavitation number, and aspect ratio is

$$c = 0.59 - 1.325\sigma + 0.0825\ AR\sigma \qquad \text{for} \qquad 2.5 < AR < 6 \tag{16}$$

The solid line shown on each of the plots in Fig. 7 is the line given by Eq. (16).

It should be mentioned that the towing tank tests were conducted at relatively low velocities and high ambient pressures. Therefore, σ_v was relatively large (about 6 to 12). Since σ was generally small (< 0.3), the term $1 - \sigma/\sigma_v$ was approximately unity. To determine the validity of Eq. (11) under conditions for which σ_v was not large, higher velocities or lower ambient pressures than could be obtained in the towing tank were required. It was thus decided to make a comparison with a previously determined empirical equation presented in an earlier report summarizing data taken in a free-jet water tunnel [5]. The equation for the reentrant-jet region was

$$W = KA(0.9 - \sigma/\sigma_v) \sin\alpha \tag{17}$$

where K = a constant, either 4.8×10^{-4} or 8.6×10^{-4} depending on σ_v,
α = angle of attack, and
A = foil area in sq inches.

If this air-flow rate is set equal to that in Eq. (11) and measured values of C_D from the free jet are used, it is possible to reduce the data in terms of the concentration c for a lower range of σ_v. Results of this reduction for a foil with infinite aspect ratio are shown in Fig. 7f. The values tend to be higher than those obtained in the towing tank, although the

slopes of the lines are nearly the same. However, it must also be mentioned that the direction of the gravity field relative to the longitudinal axis of the cavity was different in the two facilities. Observations of the reentrant jet revealed that in the vertical free-jet experiments, the reentrant jet impinged on both walls of the cavity, whereas in the towing tank only the lower surface of the cavity wall was struck by the falling reentrant jet.

Furthermore, it will be noted from Eq. (11) that the air entrainment is a function of velocity for a given σ. Figure 8 shows the variation of air entrainment with velocity for several cavitation numbers and a fixed ambient pressure on a particular hydrofoil. For a given σ, the air entrainment increases with velocity to a maximum, and then decreases to zero as the velocity approaches that required to have natural cavitation of the same degree.

At the lower velocities, the velocity for a given ambient pressure was not sufficient to permit the formation of a natural cavity. The cavity was forced by the introduction of gas into the region. Thus, the partial pressure of the air in the cavity was dominant over the partial pressure of the water vapor. However, as the velocity increases, the contribution of the partial pressure of the water vapor to the total cavity pressure increases until eventually the point will be reached where no air is required to maintain a given σ. The curves shown in Fig. 8 were based on data taken in the towing tank at atmospheric pressure and velocities less than 20 fps, i.e., for velocities less than the critical velocity at which maximum entrainment occurred. The data taken in the free-jet water tunnel were taken at higher velocities and lower ambient pressures, but the range was still not sufficient to cover a region through the critical velocity. Thus, in an effort to determine the general validity of the curves, a brief test was conducted in a closed water tunnel where it was possible to achieve the desired conditions. Results for a circular cylinder are shown in Fig. 9 for two cavitation numbers. Since the lack of a dynamometer in this facility prevented determination of the drag coefficient, the concentration factor was not calculated. Thus, the curves shown in Fig. 9 are not calculated, but are simply drawn to best fit the experimental data. Note that the shape of the curves is essentially the same as that predicted by Eq. (11) and plotted in Fig. 8, thereby qualitatively verifying the analysis.

D. Cavity Length and Planform

Studies were made of cavity length and planform by taking photographs from directly above the cavities. From these photographs, cavity lengths were measured and typical results are shown in Fig. 10. The cavity length was measured from the leading edge of the foil. As the cavity length was rather difficult to define accurately in many cases, considerable scatter may be expected in the results.

It may be concluded from an examination of the curves that for reentrant-jet cavities the cavity length was nearly independent of submergence, velocity, angle of attack, and aspect ratio, and directly proportional to the chord length.

In the pulsating-trailing vortex region, at the lower cavitation numbers there seems to be a slight effect of aspect ratio and very definite effects of submergence and angle of attack. In general, for this type of cavity it was found that for a constant σ the cavity length decreased for decreasing submergence, aspect ratio, and angle of attack.

It is interesting to note that Kermeen's [11] tests in a closed-jet water tunnel also showed a similar dependence on aspect ratio and angle of attack well into the reentrant-jet region.

Of particular interest was the variation of the width of the reentrant jet itself with aspect ratio. Figures 11, 12, and 13 show typical photographs of the cavity planform and reentrant-jet shapes at various air-supply rates for the three aspect ratios tested (i.e., 2.5, 4, and 6). The change in mode of air entrainment can also be noted. Associated with each set of photographs, an air-demand curve relates the position of each individual photograph on the curve by the letter adjacent to each point on the graph.

It appears that, as the aspect ratio increases, the reentrant jet occupies relatively less of the cavity width (i.e., the reentrant jet deviates more from the two-dimensional pattern as the aspect ratio increases). More complete investigation should be made of this behavior.

It is also interesting to note the several sets of trailing vortices which accompany the relatively long reentrant-jet cavities and the pulsating cavities, particularly for the foils with aspect ratio 4 and 6. These vortices appear to extend over the region of the cavity not covered by the

reentrant jet, and possess some symmetry with respect to the longitudinal axis of the cavity. The photographs presented by Kermeen also exhibit these trailing vortices for the larger aspect ratios investigated. It is clear from his data that, since the measured σ's were less than the calculated σ_v's, air was present in the cavity although the source of this air is not known.

E. Cavity Stability

Cavities which release air by entrainment in the reentrant jet and through trailing vortices are steady cavities, i.e., the shape does not change with respect to time. Pulsating cavities, on the other hand, are unsteady. The existence of instability or pulsation at the higher air-flow rates is evidenced by cavity pressure fluctuations or relatively high amplitudes and low frequency (40 cps to 60 cps), definite transverse waves appearing on the cavity surface, and an audible sound emanating from the cavity.

This pulsation phenomenon in the cavity free-jet system has been described at length by Silberman and Song [5]. It has also been reported by Wetzel and Schiebe [1] for tests conducted in a towing tank. In a more recent paper, Song [8] considered a mass-compliance model of a cavity free-jet system.

The conclusions drawn from this theoretical analysis were as follows:

(1) One or more free surfaces are required for the pulsation phenomena to exist unless the fluid is compressible.

(2) The phenomenon is one of resonance in which the resonant system is the large bubble clinging to the back of a hydrofoil and the sustaining energy is being supplied by the flow past the foil-cavity system.

(3) There may be any integral number of waves appearing on a cavity wall. The cavities may be classified according to the number of wave lengths appearing on the cavity wall and called first-stage, second-stage, etc.

(4) To each number of stages there corresponds a definite amplitude of pulsation and maximum air-carrying capacity.

(5) Both frequency and amplitude of pulsation are very insensitive to air-supply-rate change.

(6) The Strouhal number based on cavity length ℓ_c, cavity wall velocity V_c, and frequency of pulsation f, is equal to the number of stages or wave lengths appearing on the cavity wall n.

$$\frac{f\ell_c}{V_c} = n \tag{18}$$

(7) An equation useful for correlating data for pulsating cavities was given as

$$\sigma_v = (1 + 3.45n^2)\sigma + 3.45n^2\sigma^2 \tag{19}$$

where σ_v = cavitation number based on vapor pressure,
n = number of stages, and
σ = cavitation number.

Observations and measurements obtained in the towing tank generally confirm these conclusions. There are some definite observations, however, which should be mentioned.

In certain cases, there seemed to be a change in the number of stages as the quantity of air injected into the cavity was increased. In general, however, the mode of air release shifted from the pulsating cavity to the trailing-vortex cavity without shifting the number of stages as the air rate was increased. In this case, the frequency of pulsation was relatively insensitive to air-supply rate. There was only a slight decrease in frequency with increasing air-supply rate with no apparent change in number of stages. In contrast, frequency measurement in the free jet showed practically no variation in frequency with changes in air-supply rate unless the number of stages changed.

The data for the amplitude of the pressure pulsation obtained in the towing tank were somewhat limited. The only way that the amplitude of pulsation could be measured was by introducing a pressure transducer directly in the cavity. This proved to be inconvenient, except for the flat plate of 4-in. chord. However, the trend of the available data qualitatively showed that the amplitude was relatively insensitive to a change of air-supply rate.

As a typical example of the magnitude of these features, a pulsating cavity on a 0.1- by 2-degree Tulin Hydrofoil of aspect ratio 2, operating at 3-chords submergence and at a velocity of 14 fps, was investigated. The cavity had approximately six wave lengths or stages and a frequency of pulsation of 56 cps. The peak-to-peak pulsating pressure amplitude within the cavity was 0.35 ft of water. The observed wave form of the cavity pressure was very nearly a pure sinusoid. Preliminary measurements made by placing a hydrophone in the towing tank 4 ft below the cavity indicated that as the cavity passed over the hydrophone the radiated sound was in excess of 116 microbars. Thus, a pulsating cavity was an intense source of low-frequency sound in water.

It was indicated in the last section that for pulsating cavities the cavity length shortened as the free surface was approached. This implied that, for a given velocity, cavitation number, and number of stages, the frequency of pulsation should increase according to Eq. (18) as the free surface was approached. Several calculations have shown this to be true.

In regard to Eq. (19), it should be mentioned that the numerical constant, 3.45, was determined empirically from conditions in the free-jet water tunnel. It was shown that this constant was a function of the jet width and the ratio of the portion of cavity volume filled with gas to the portion filled with water and water vapor. This ratio can be easily shown to depend upon velocity by analysis presented earlier in this paper. Therefore, the constant for other conditions, such as those present in the towing tank, would be expected to be different. Also, the relationship required between cavity area and σ in Eq. (19) was determined from theory for flow about a thin wedge. Other shapes may alter the form of the equation to some extent. For comparative purposes, Fig. 14 shows towing-tank data for a flat plate foil and lines represented by Eq. (19) plotted on log-log scales. The discrepancy noted is probably due to the functional relationship of the numerical factor with submergence or jet width in Eq. (19) which was not taken into consideration. It should also be emphasized that the accuracy of determining the number of stages from photographs is plus or minus one stage. Equation (19) cannot be used to predict the inception of pulsation until it is possible to determine the number of stages for given initial conditions. This as yet has not been completely determined.

It was noted that under some operating conditions the cavity would change from a reentrant-jet cavity to a pulsating cavity as the air-injection

rate was increased and finally, at very high injection rates, to a cavity with trailing vortices. It was also noted that under some conditions the cavity would change from reentrant-jet conditions to trailing-vortex conditions without pulsations of the cavity occurring at any time. For example, as the angle of attack was increased, the tendency was for the cavity to develop trailing vortices rather than to lose air by pulsation.

It can be seen from the work of Cox and Clayden, and Campbell and Hilborne, that the thickness of the cavity plays an important role in determining the strength of the circulation around the cavity set up by gravitational forces. The actual thickness of the cavity was not measured in the tests and a more indirect method was utilized to determine its effect on stability.

A brief series of tests was conducted to determine the conditions under which the mode of entrainment would change directly from a reentrant jet to trailing vortices without experiencing any pulsation or instability as the air-injection rate was increased.

At high angles of attack, trailing vortices have been observed at the rear of the cavity whereas at the lower angles pulsation of the cavity generally occurred for the high air-flow rates. Thus, for given conditions, a critical angle existed that determined which type of entrainment would actually occur. Typical preliminary data of this type are summarized in Fig. 15. The curves shown in Fig. 15 are drawn through these critical angles. For the foil placed at an angle of attack that lies under the curves, the cavities would pulsate when sufficient air was injected. For angles above the curves, the cavity had trailing vortices and would not pulsate for any air-supply rates. It can be seen from Figs. 15b and 15c that as the velocity and chord length increase the critical angle decreases. If this trend continues for prototype conditions, pulsation may not occur.

As the foil approaches the free surface, the critical angle decreases and the tendency to pulsate decreases. It is also apparent that cavity characteristics for the low-aspect-ratio foils are conducive to cavity pulsation. From the limited amount of data, it appears that for increasing aspect ratio the critical angle also increases slightly. Future investigation may reveal that an optimum aspect ratio may be found for which the cavity is least likely to pulsate.

It should be mentioned that these latter tests are not conclusive and more data are required to completely define the phenomena.

F. Force Measurements

There has been considerable effort devoted to the determination of hydrodynamic force characteristics of a submerged three-dimensional hydrofoil operating with a finite σ. Wu [12] has calculated force coefficients for two-dimensional hydrofoils in an infinite fluid for an arbitrary σ. In principle, this method can be used for any arbitrary profile; however, it is extremely complicated for sections other than simple flat plates and circular arcs.

Johnson [13] has developed a theory for the force characteristics for three-dimensional hydrofoils of arbitrary section at finite submergences for $\sigma = 0$. He has conducted experiments that have verified this theory and has also shown that the cavity shape and hydrodynamic characteristics are essentially independent of the gas in the cavity if the cavitation number based on cavity pressure remains the same. The data from these experiments consisted of photographs and force measurements under natural and ventilated conditions.

Cumberbatch [14] has theoretically considered the tip effects on the cavitating flow past a large aspect-ratio lifting hydrofoil. The two-dimensional lift coefficient, as determined from Wu, was thus modified to give the three-dimensional lift coefficient in an infinite fluid for a finite σ.

Johnson's calculations can be reduced to Wu's for a two-dimensional hydrofoil in an infinite fluid at $\sigma = 0$. However, Cumberbatch's theory cannot be reduced to Johnson's values at $\sigma = 0$ as several assumptions are no longer valid in that case. Cumberbatch has made comparisons with the experimental work of Kermeen [11] with correlation being obtained for the moderate aspect ratios (< 4) and values of $\sigma > 0.1$.

A comparison of St. Anthony Falls experimental data and calculated force coefficients using Johnson's and Cumberbatch's theories is shown in Fig. 16 for a flat plate foil with an aspect ratio of 2.5. In these plots, Cumberbatch's theory was used for cavitation numbers down to 0.04, although the theory is probably not valid for such small σ. However, the computation serves to emphasize the difference between the two theories at the small σ. Experimental data for the foil at angles of attack of 12, 16, and 20 degrees

are also shown. As Cumberbatch's theory was derived for an infinite fluid, the comparison is made with data taken for the foil at a submergence of 3 chords, thereby approaching the infinite-fluid case. It can be seen from Fig. 16a that the experimental and calculated lift coefficients agreed well for the higher σ's, the agreement with Cumberbatch's solution deteriorating at the smaller σ as expected. The data can reasonably be extrapolated to agree with theory at $\sigma = 0$. Figure 16b indicates that the drag coefficient can apparently be predicted with good success (the legend is the same as for Fig. 16a). The calculated drag coefficient was obtained from the tangent rule ($C_D = C_L \tan \alpha$) for all σ's where the length of the cavity exceeded the chord length. This relation assumed that the contribution of skin friction on the lower surface of the hydrofoil to the total drag was small.

Figures 17, 18, and 19 show additional force-coefficient data for three aspect ratios and submergence ratios for a flat plate foil. The points at $\sigma = 0$ were calculated using Johnson's theory. The lines through the data for $\sigma > 0$ and each angle of attack were drawn to best fit the data and are not theoretical curves. A larger number of data points were available to determine the location of this line than are shown in these figures. Some of the points were intentionally omitted to prevent excessive confusion of points on the small graph. The strut drag has been subtracted from the total drag before reducing the data in the form of a drag coefficient. In most cases, it will be seen that submergence has very little effect on the force coefficients.

It was also possible to compare data with that reported by Kermeen for a particular aspect ratio. This comparison is shown in Figs. 18e and 18f for an aspect ratio of 4. The agreement appears to be satisfactory. St. Anthony Falls data at a submergence of two chords were used in this comparison as little effect of submergence was noted.

Data for the largest aspect ratio available are shown in Fig. 19. It will be noticed that in this case the angles of attack were different from those for the previous two aspect ratios. During the course of the tests for this particular foil, it was found that the device used to measure the angle of attack was displaced by 1.5 degrees from its original zero position. Thus, rather than repeat the experiments at the same nominal angles previously used, it was decided to present the data in the form shown for comparison purposes.

V. CONCLUSIONS

Based on the experimental data taken for ventilated cavities, it is possible to draw the following conclusions:

(1) Forced ventilation at low angles of attack can be more easily obtained by introducing a small quantity of air in the region of the leading edge of a foil. Larger quantities of air may be introduced along the span at essentially any chord-wise position. For higher angles of attack, the supplementary air supply is not required.

(2) For reentrant jet cavities, the main source of air entrainment is the reentrant jet itself. Therefore, the concentration of air entrained in the reentrant jet is a suitable correlation factor for ventilated cavities. Air-entrainment rates for a hydrofoil of rectangular planform can be determined from Eqs. (11) and (16) for aspect ratios of 2.5 to 6.

(3) In general, instability of the cavity was observed for the relatively thin cavities. The high σ_v inherent to the towing tank (high ambient pressures and low velocities) restricted the form of pulsation to a large number of waves or stages. As the foil was brought closer to the free surface, the frequency of pulsation and the cavity length varied essentially as that given by Eq. (18). The conditions necessary for the prediction of pulsation have not yet been completely defined.

(4) Experimental force data indicated only a slight influence of the free surface. Results of data extrapolated to $\sigma = 0$ agreed satisfactorily with theory developed by Johnson [13]. Correlation of data with theory by Cumberbatch [14] was found at the higher cavitation numbers. Close agreement with force data taken in a closed water tunnel by Kermeen [11] was obtained for the finite-span flat plates.

LIST OF REFERENCES

[1] Wetzel, J. M. and Schiebe, F. R. Experimental Studies of Artificial Cavities on Submerged Hydrofoils of Finite Span. University of Minnesota, St. Anthony Falls Hydraulic Laboratory Memorandum No. M-89, Minneapolis, Minnesota. November 1960. Not available for distribution.

[2] Schiebe, F. R. and Wetzel, J. M. Ventilated Cavities on Submerged Hydrofoils of Finite Span. University of Minnesota, St. Anthony Falls Hydraulic Laboratory Memorandum No. M-91, Minneapolis, Minnesota. July 1961. Not available for distribution.

[3] Cuthbert, Jerry W. An Analysis of Air Entrainment in Cavity Flows. Hydronautics, Incorporated, Technical Report 003-1, Rockville, Maryland. October 10, 1960.

[4] Birkhoff, Gattett. Hydrodynamics, First Edition, Dover Publications, Incorporated, New York. p. 75.

[5] Silberman, E. and Song, C. S. Instability of Ventilated Cavities. University of Minnesota, St. Anthony Falls Hydraulic Laboratory Technical Paper No. 29-B, Minneapolis, Minnesota. November 1959.

[6] Song, C. S. Pulsation of Ventilated Cavities. University of Minnesota, St. Anthony Falls Hydraulic Laboratory Technical Paper No. 32-B, Minneapolis, Minnesota. February 1961.

[7] Swanson, W. M. and O'Neill, J. P. The Stability of an Air-Maintained Cavity Behind a Stationary Object in Flowing Water. California Institute of Technology, Hydrodynamics Laboratory (unpublished).

[8] Cox, R. N. and Clayden, W. A. "Air Entrainment at the Rear of a Steady Cavity," Proceedings of N. P. L. Symposium on Cavitation in Hydrodynamics. London, H. M. S. O. 1956.

[9] Campbell, I. J. and Hilborne, D. V. "Air Entrainment Behind Artificially Inflated Cavities," Second Symposium on Naval Hydrodynamics, Washington, D. C. August 25-29, 1958.

[10] Lamb, Owen P. and Killen, John M. An Electrical Method for Measuring Air Concentration in Flowing Air-Water Mixtures. University of Minnesota, St. Anthony Falls Hydraulic Laboratory Technical Paper No. 2-B, Minneapolis, Minnesota. March 1950.

[11] Kermeen, R. W. Experimental Investigation of Three-Dimensional Effects on Cavitating Hydrofoils. California Institute of Technology, Engineering Division Report No. 47-14, Pasadena, California. September 1960.

[12] Wu, T. Yao-Tou. "A Free Streamline Theory for Two-Dimensional Fully-Cavitated Hydrofoils," Journal of Mathematics and Physics, Vol. XXXV, No. 3. October 1956.

[13] Johnson, Virgil E., Jr. Theoretical and Experimental Investigation of Arbitrary Aspect-Ratio, Supercavitating Hydrofoils Operating Near the Free Surface. NACA RM L57116. December 12, 1957.

[14] Cumberbatch, E. Cavitating Flow Past a Large Aspect-Ratio Hydrofoil. California Institute of Technology, Engineering Division Report No. 47-12, Pasadena, California. May 1960.

F I G U R E S

(1 through 19)

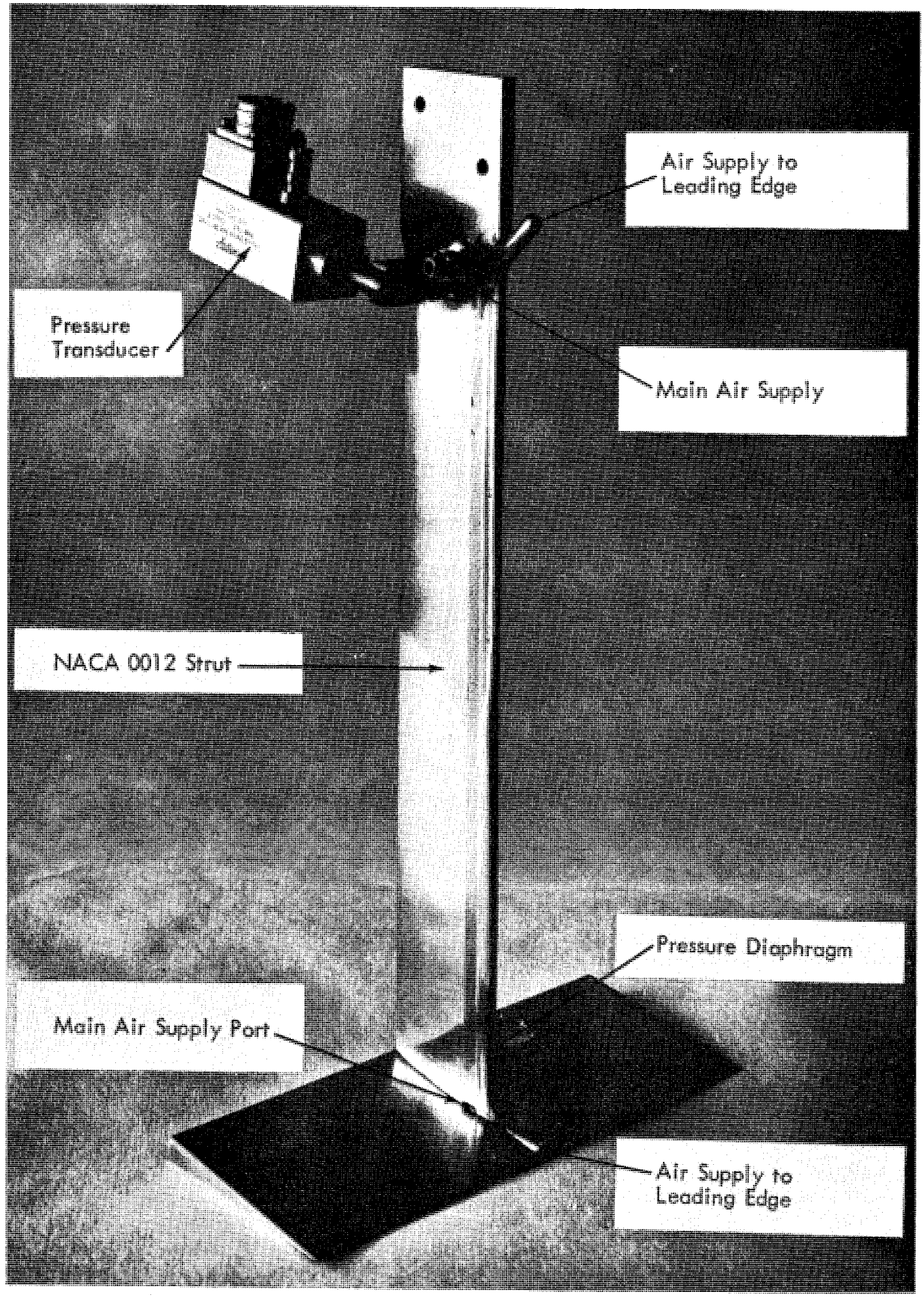

Fig. 1 - Photograph of a Typical Flat Plate Hydrofoil

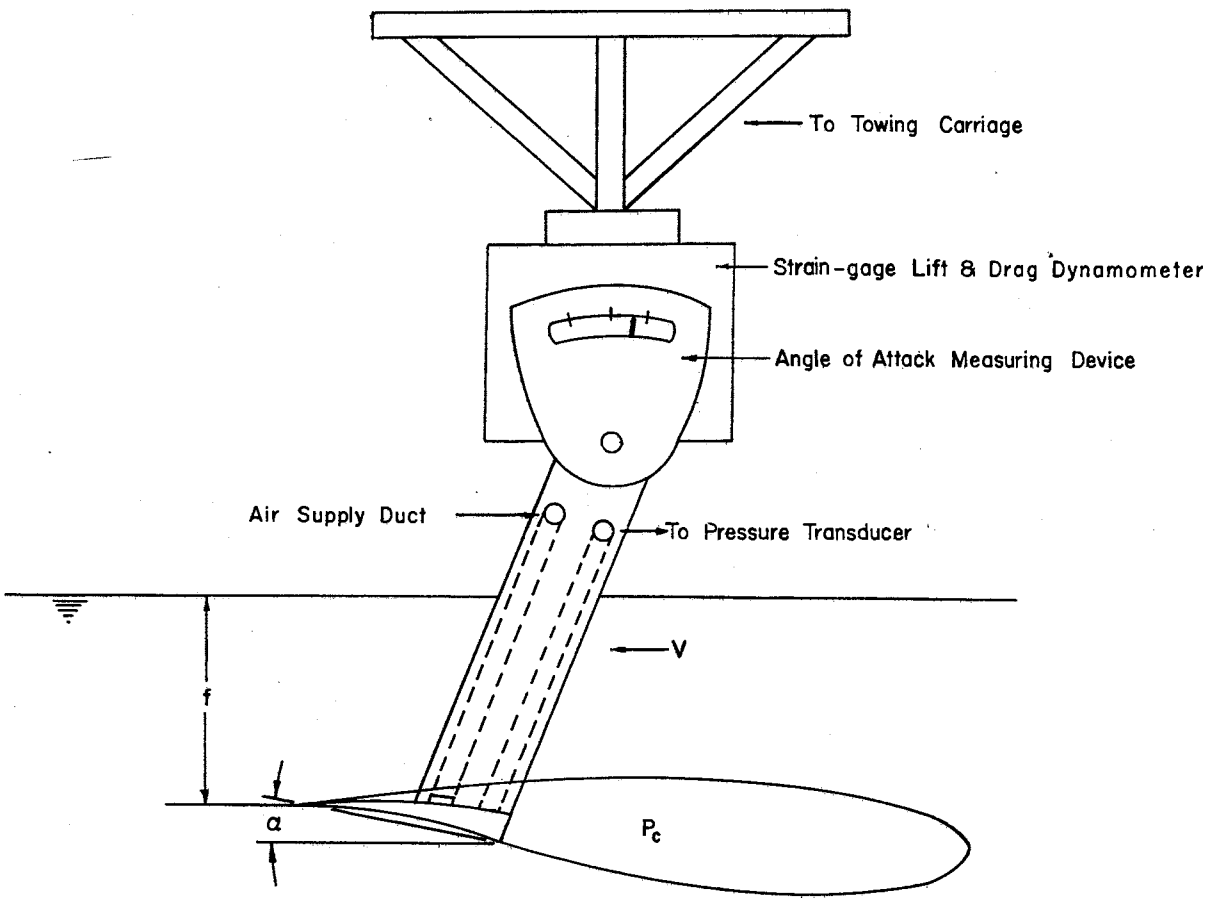

Fig. 2 - Definition Sketch

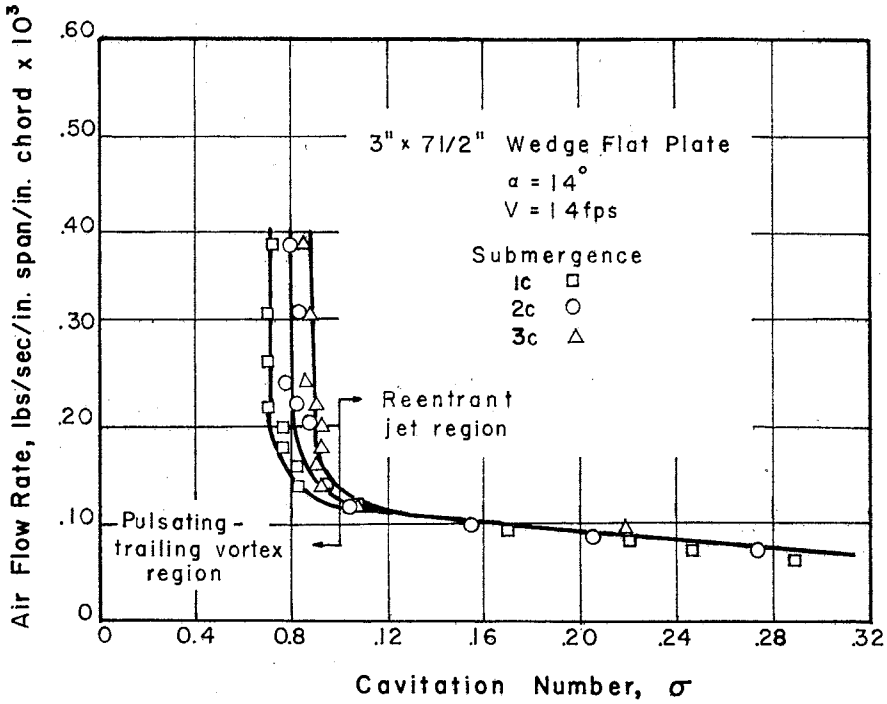

Fig. 3 - Typical Variation of Air-Entrainment Rate with Cavitation Number

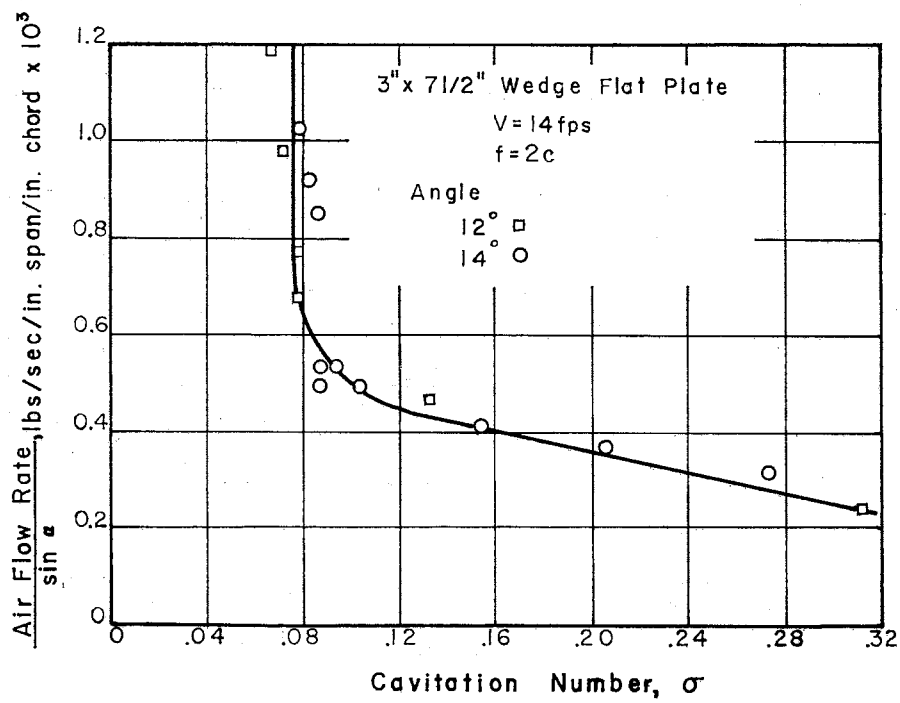

Fig. 4 - Correlation of Air-Entrainment Rate with Angle of Attack.

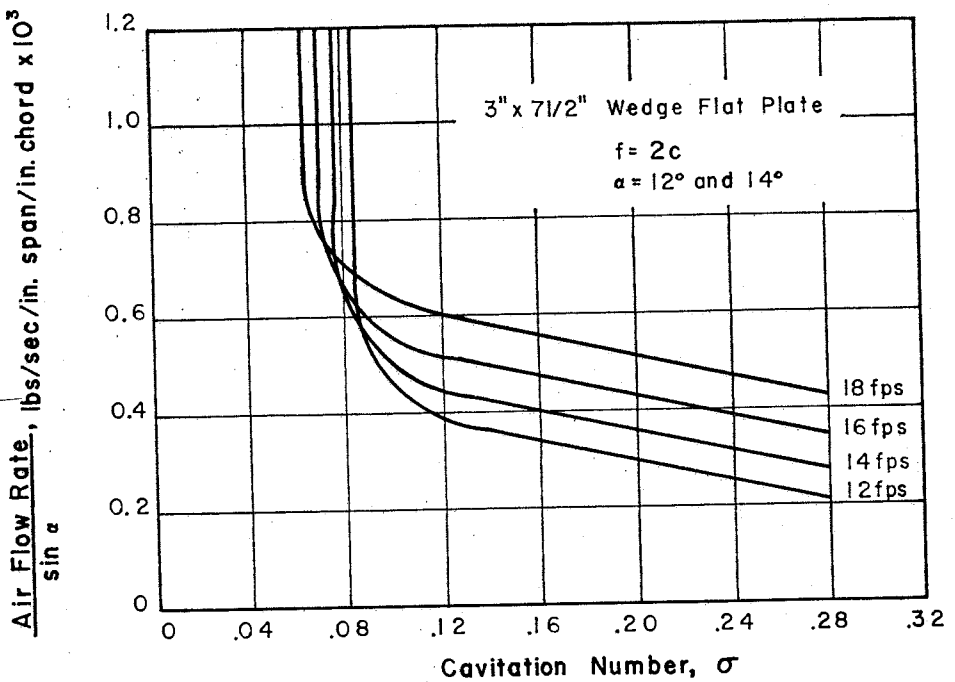

Fig. 5 – Effect of Velocity on Air-Entrainment Rates

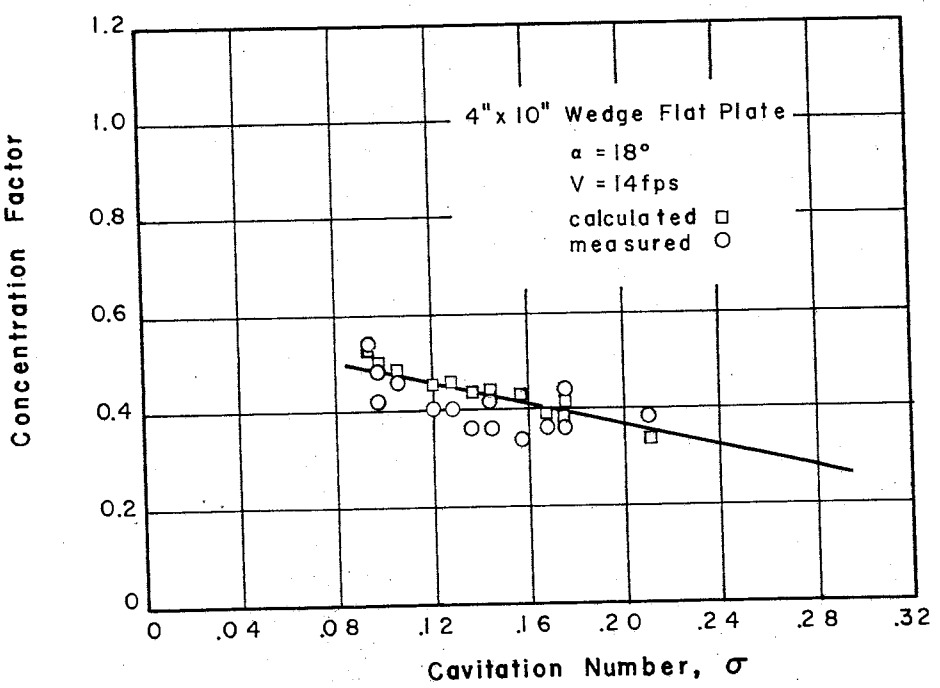

Fig. 6 – Comparison of Measured and Calculated Concentration Factors

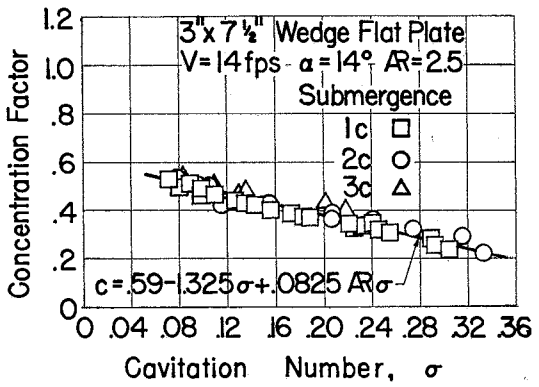

a. Effect of Submergence

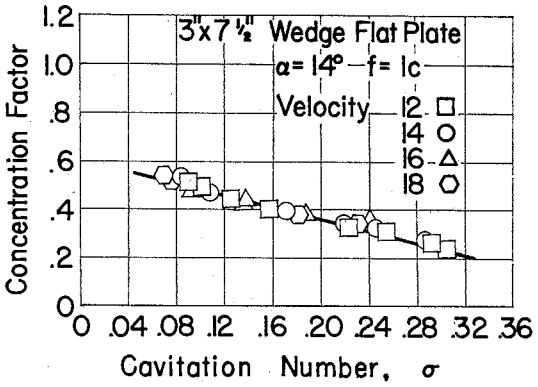

b. Effect of Velocity

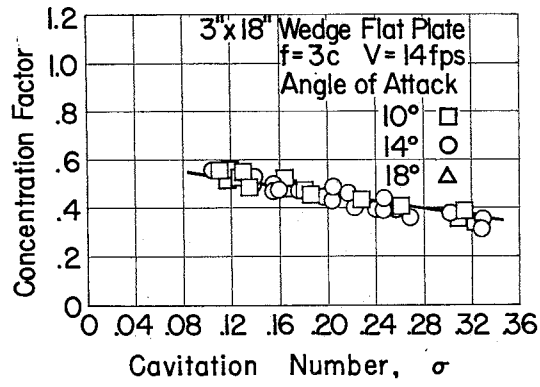

c. Effect of Angle of Attack

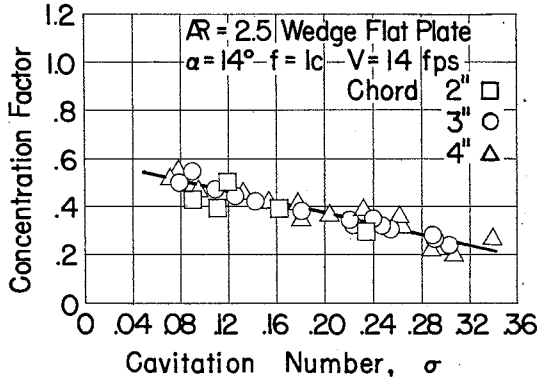

d. Effect of Chord

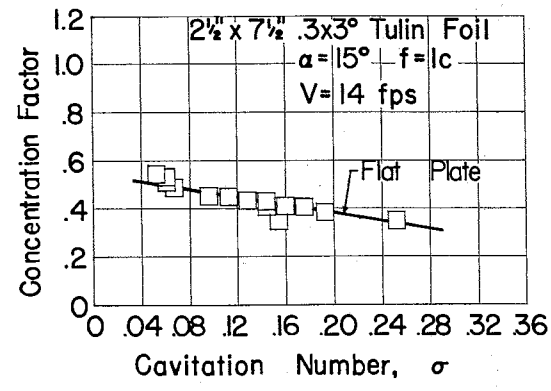

e. Effect of Camber

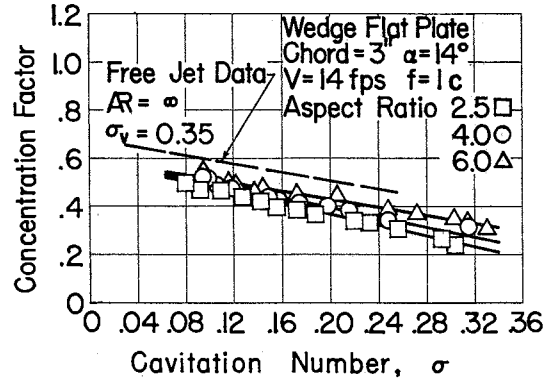

f. Effect of Aspect Ratio

Fig. 7 – Effect of Various Flow and Foil Parameters on Concentration Factor

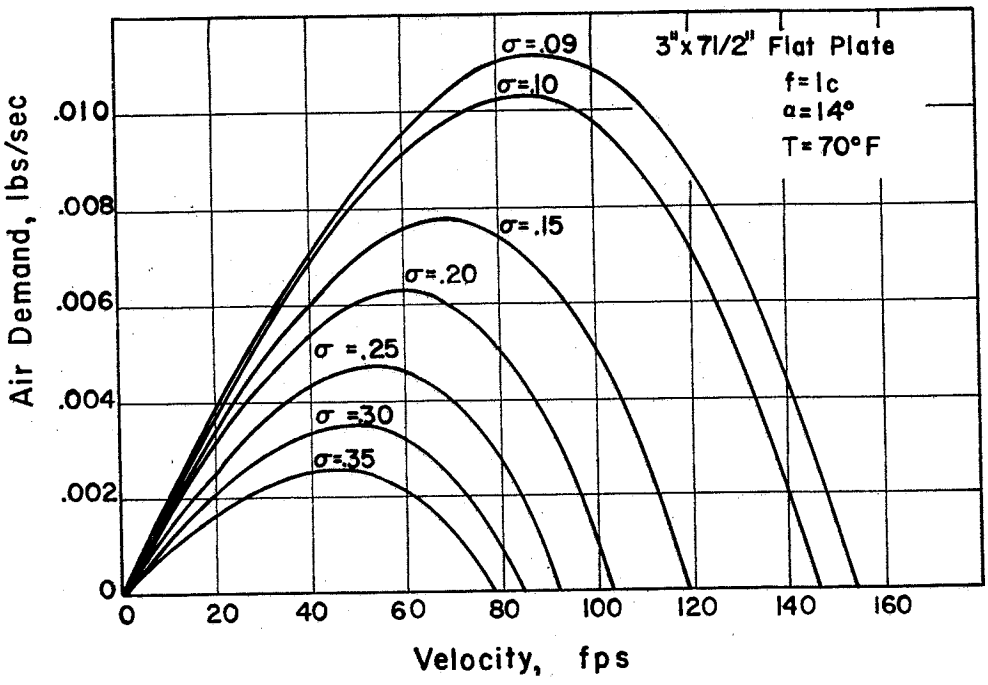

Fig. 8 - Calculated Variation of Air Demand with Velocity for Constant σ (Towing Tank)

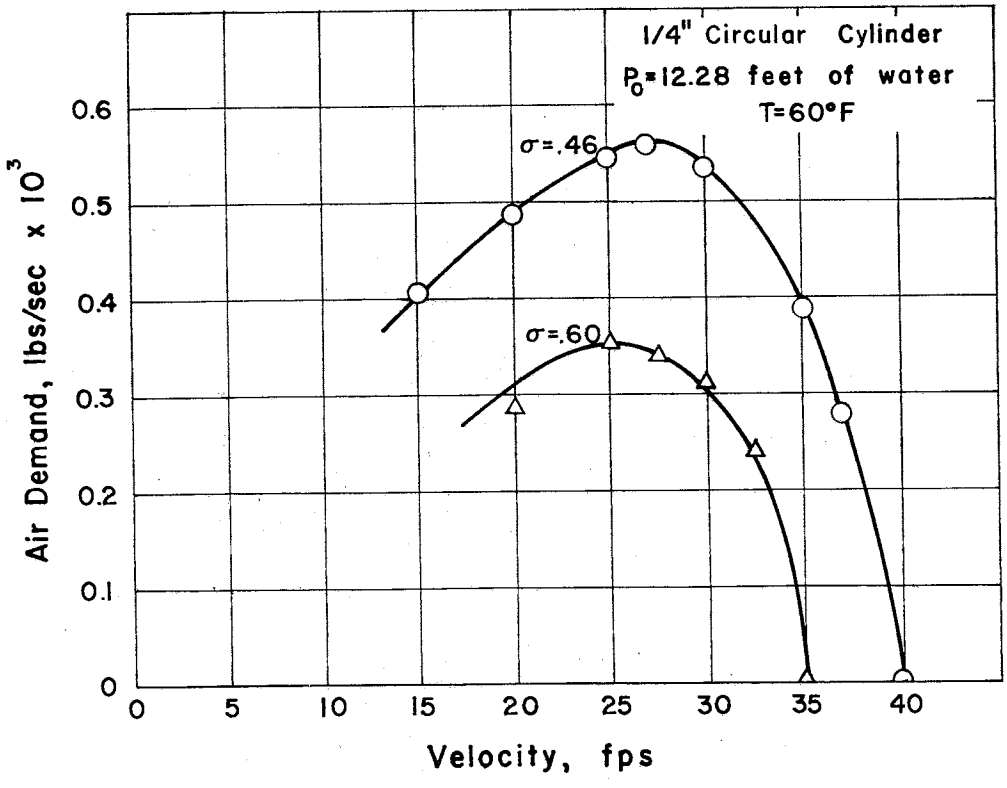

Fig. 9 - Measured Variation of Air Demand with Velocity for Constant σ (Closed Water Tunnel)

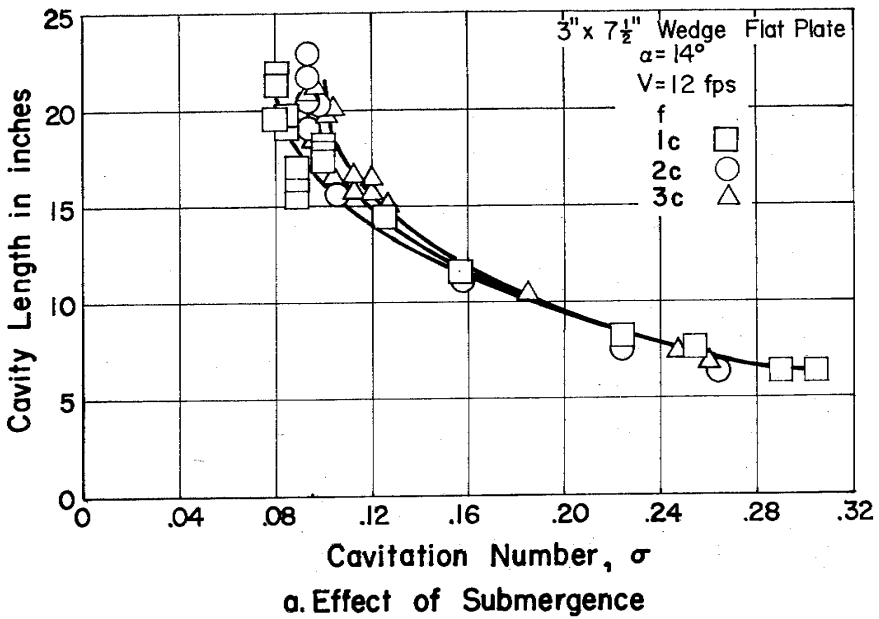

a. Effect of Submergence

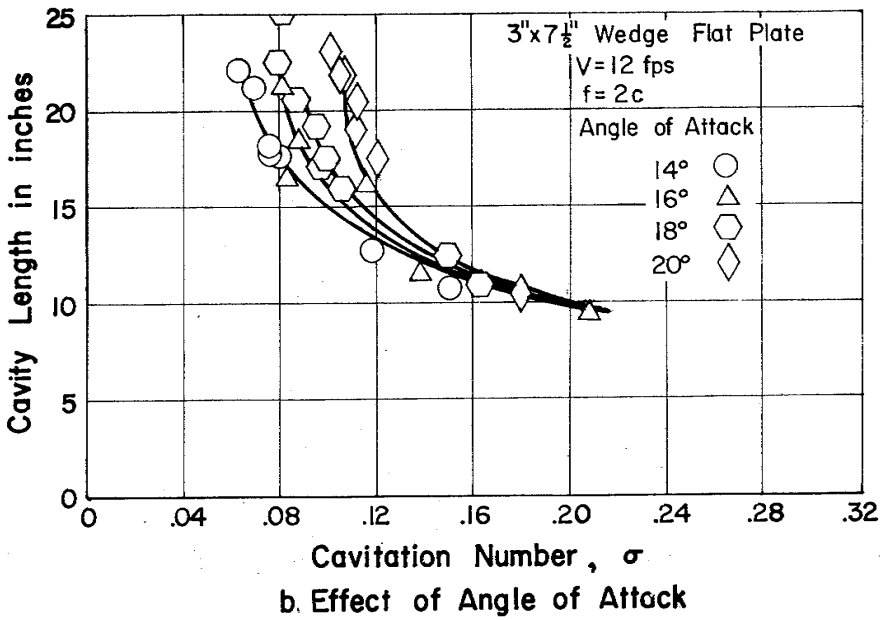

b. Effect of Angle of Attack

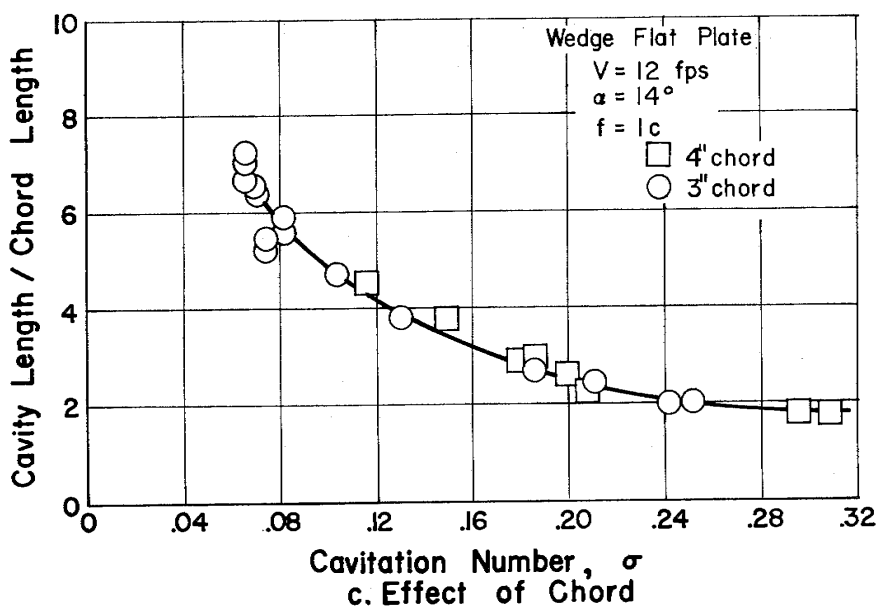

c. Effect of Chord

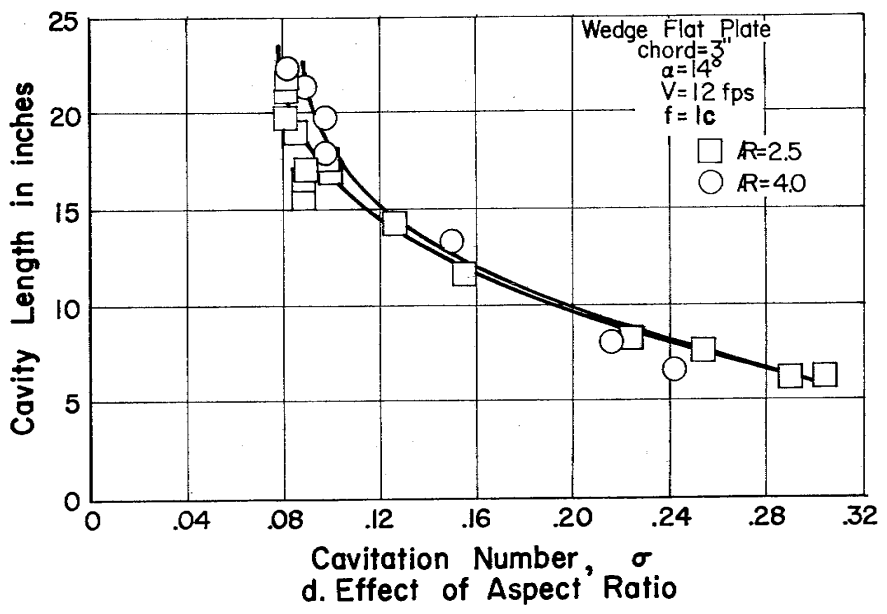

d. Effect of Aspect Ratio

Fig. 10 - Effect of Various Parameters on Cavity Length

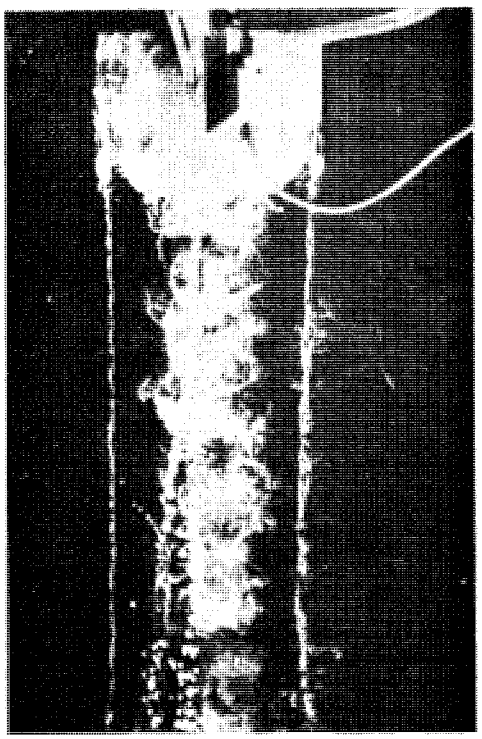

a. $\sigma = .248$ $W = 1.51 \times 10^{-3}$ lbs/sec.

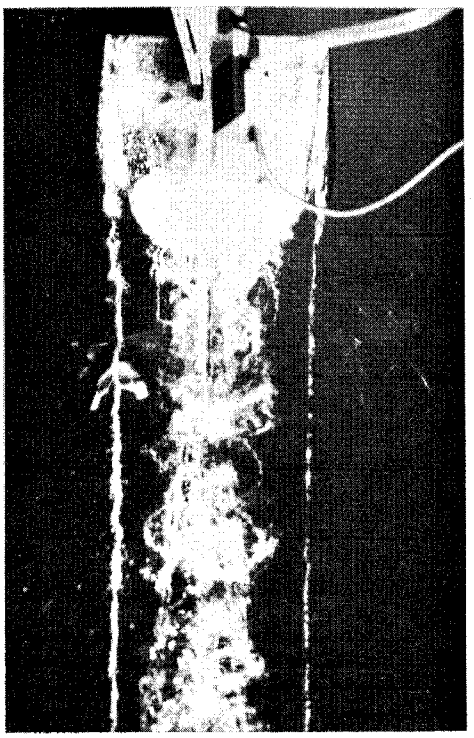

b. $\sigma = .205$ $W = 1.72 \times 10^{-3}$ lbs/sec.

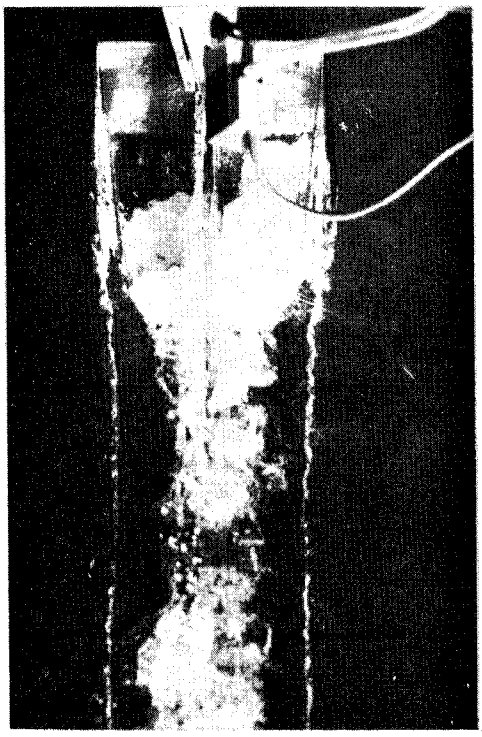

c. $\sigma = .142$ $W = 2.16 \times 10^{-3}$ lbs/sec.

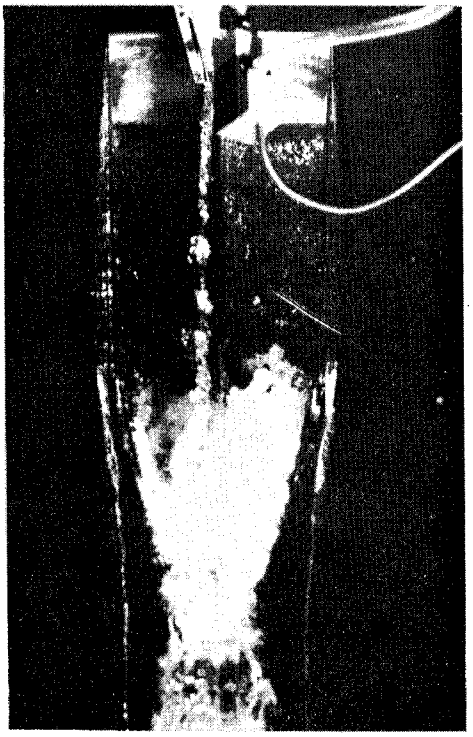

d. $\sigma = .090$ $W = 2.65 \times 10^{-3}$ lbs/sec.

Fig. 11 - Typical Cavity Photographs on Flat Plate Foil: AR = 2.5, V = 14 fps, $\alpha = 14^{\circ}$, f = 1c

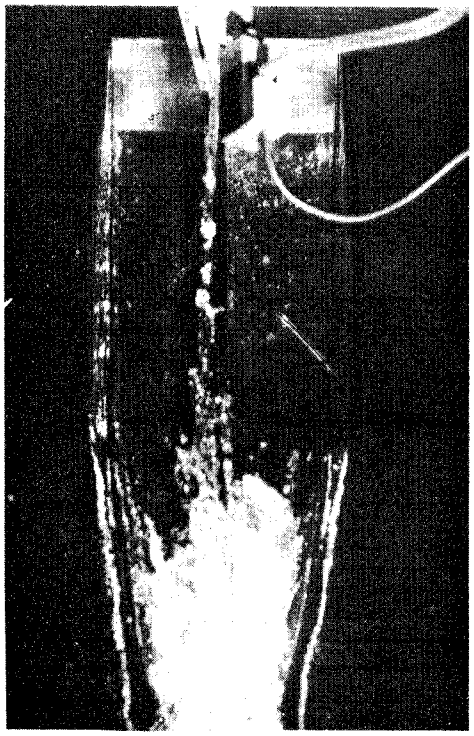

e. σ=.069 W= 3.14×10^{-3} lbs/sec.

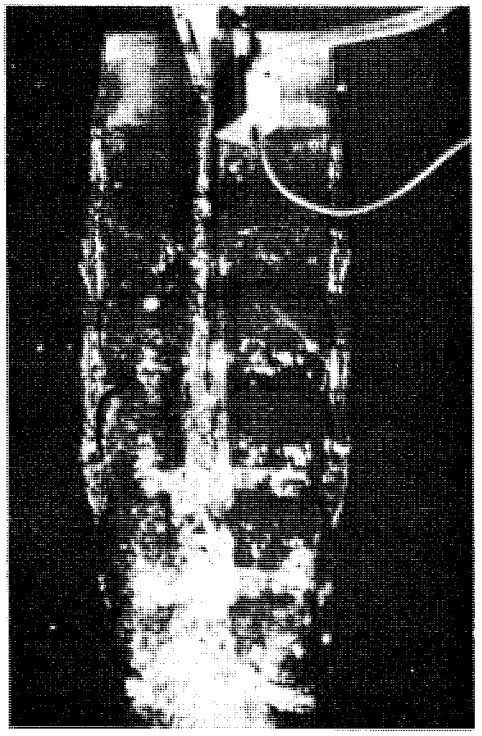

f. σ=.058 W= 5.03×10^{-3} lbs/sec.
freq=56.3cps.

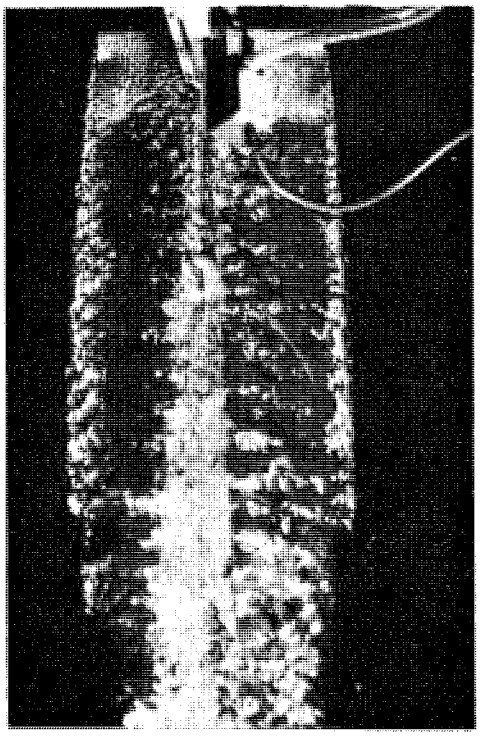

g. σ=.060 W= 8.72×10^{-3} lbs/sec.

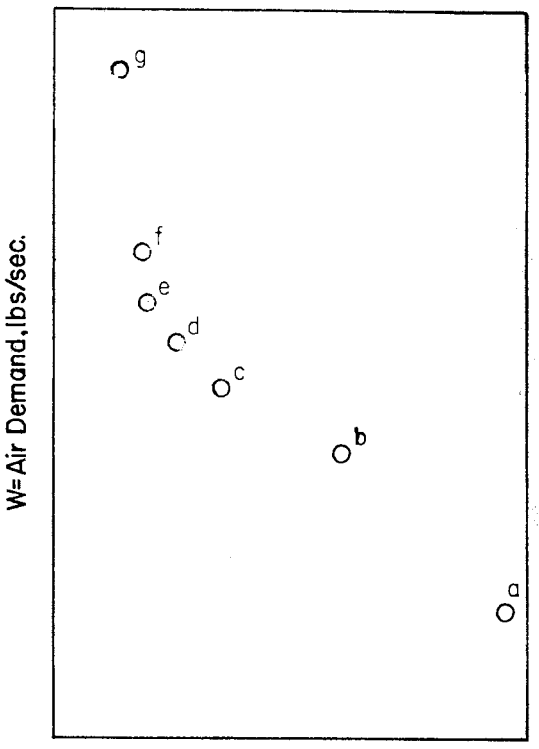

Fig. 11 cont.

a. $\sigma = .493$ $W = 1.64 \times 10^{-3}$ lbs/sec.

b. $\sigma = .315$ $W = 3.70 \times 10^{-3}$ lbs/sec.

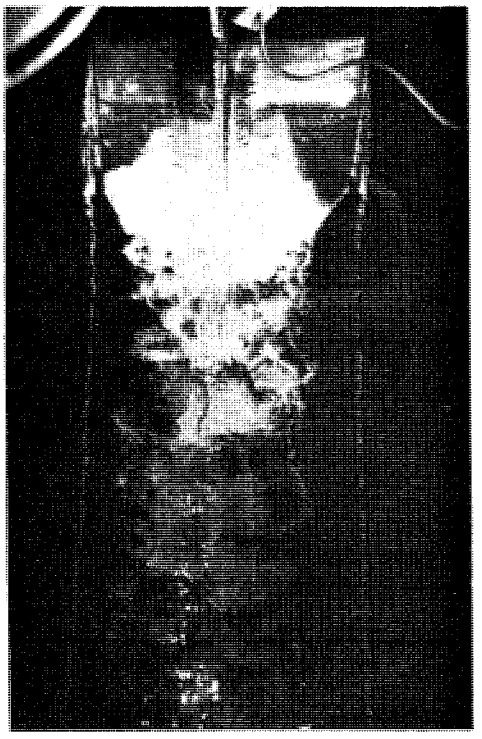

c. $\sigma = .197$ $W = 4.60 \times 10^{-3}$ lbs/sec.

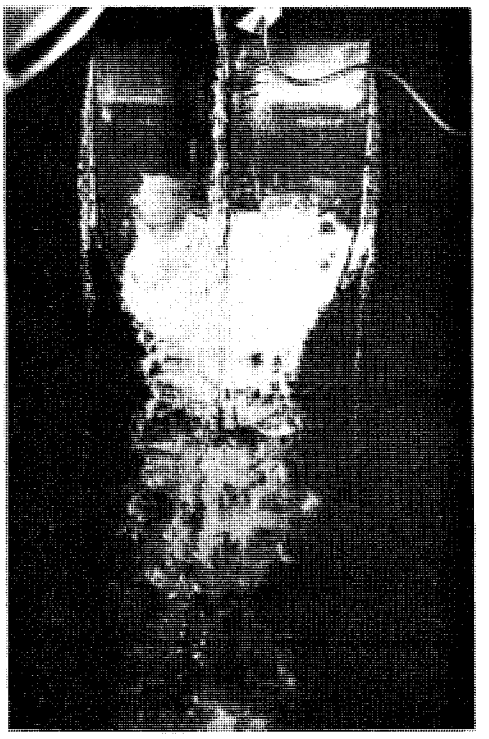

d. $\sigma = .137$ $W = 5.12 \times 10^{-3}$ lbs/sec.

Fig. 12 - Typical Cavity Photographs on Flat Plate Foil: AR = 4, V = 14 fps, $\alpha = 14^{\circ}$, f = 1c

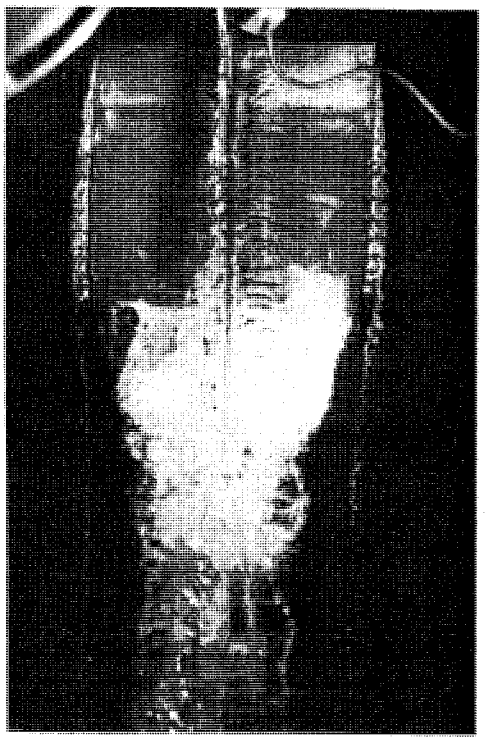

e. σ=.106 W = 5.68x10^{-3} lbs/sec.

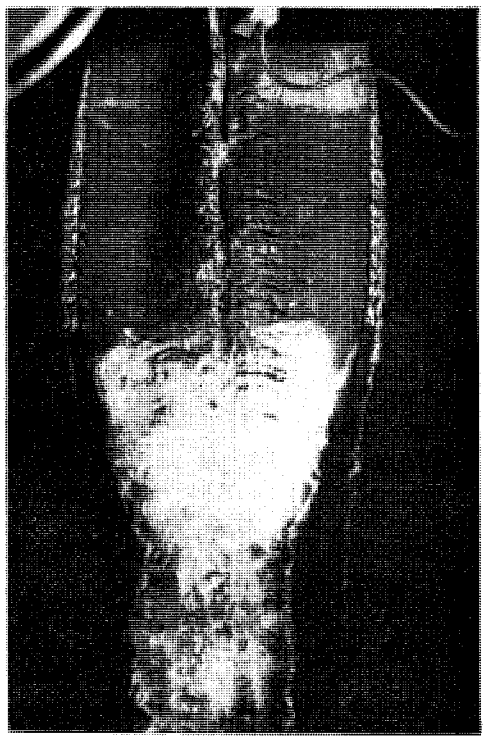

f. σ=.099 W = 6.32x10^{-3} lbs/sec.

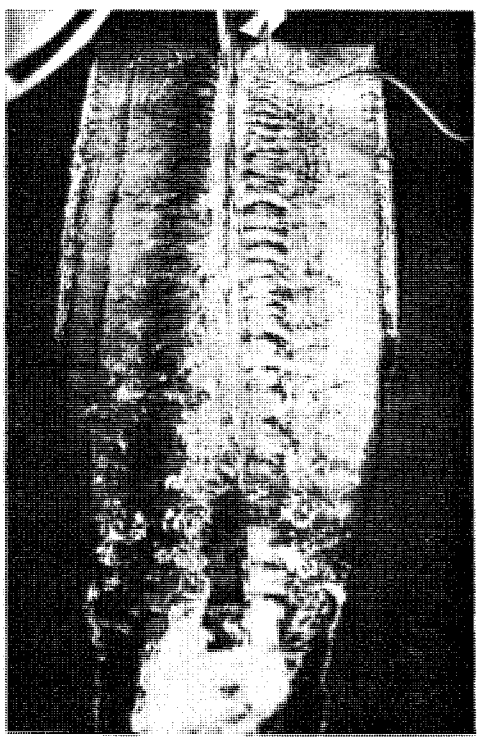

g. σ=.071 W = 8.75x10^{-3} lbs/sec.

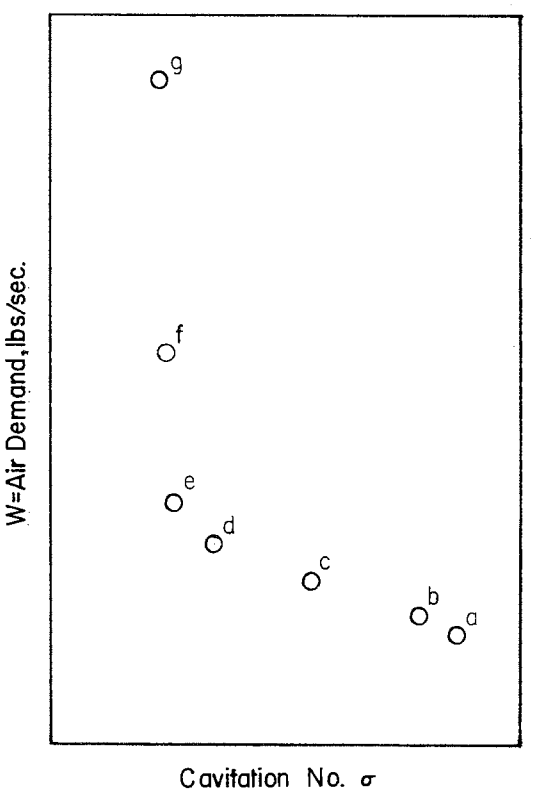

Fig. 12 cont.

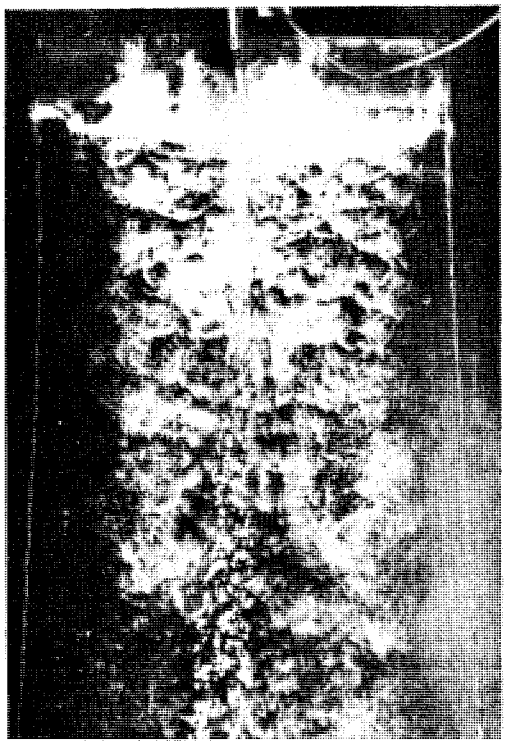

a. $\sigma = .270$ $W = 4.05 \times 10^{-3}$ lbs/sec

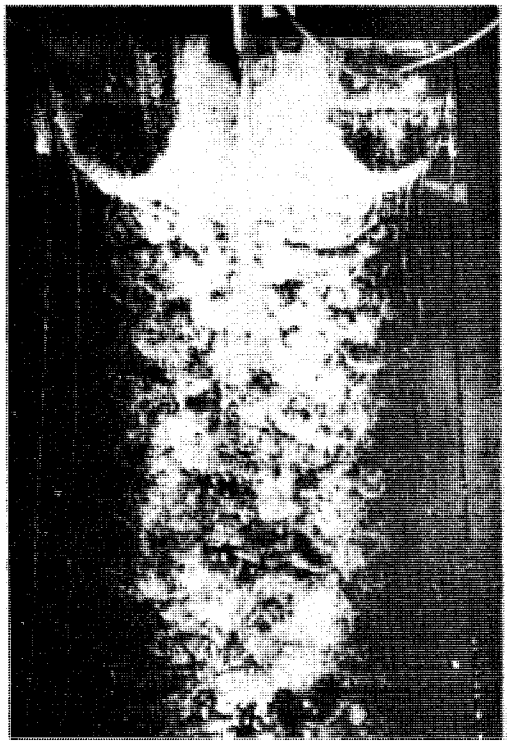

b. $\sigma = .197$ $W = 4.59 \times 10^{-3}$ lbs/sec.

c. $\sigma = .143$ $W = 5.14 \times 10^{-3}$ lbs/sec.

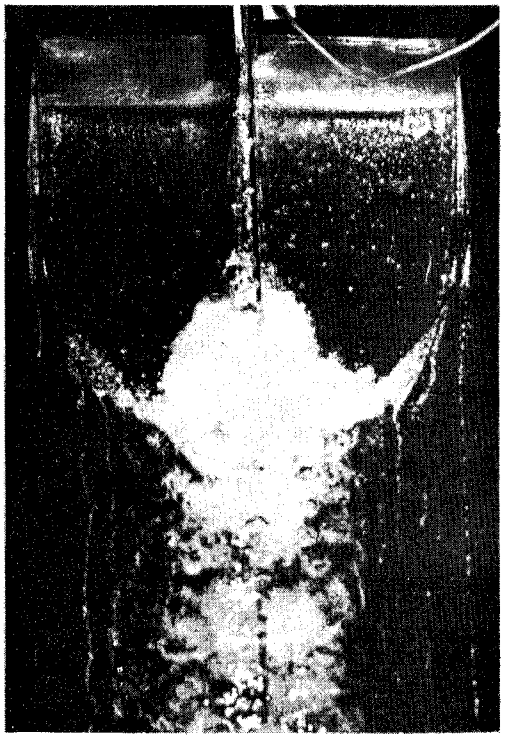

d. $\sigma = .089$ $W = 5.70 \times 10^{-3}$ lbs/sec.

Fig. 13 - Typical Cavity Photographs on Flat Plate Foil: AR = 6, V = 14 fps, $\alpha = 10^{\circ}$, f = 1c

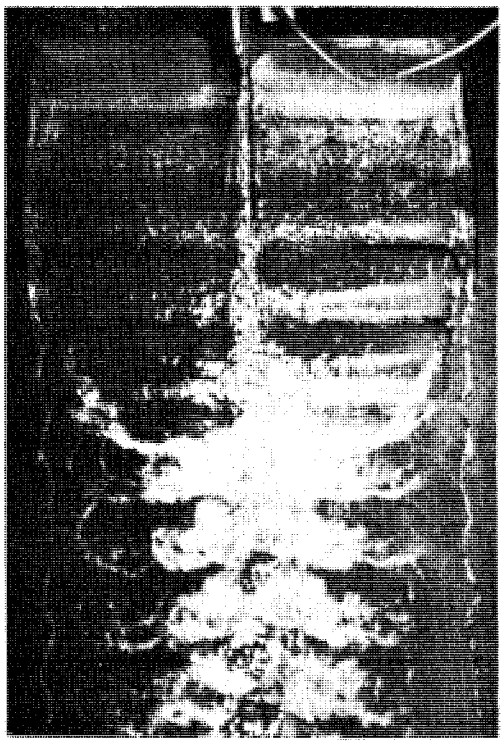

e. σ=.082 W= 6.35×10^{-3} lbs/sec.
freq= 49.8cps.

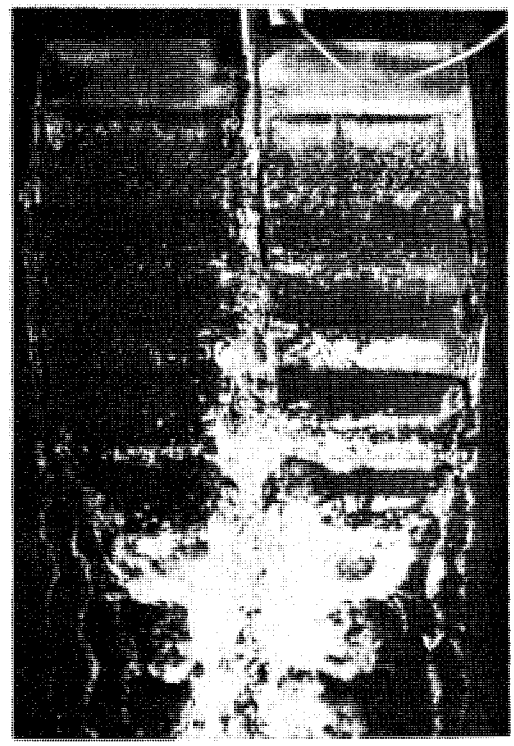

f. σ=.063 W= 7.85×10^{-3} lbs/sec.
freq=44.3cps.

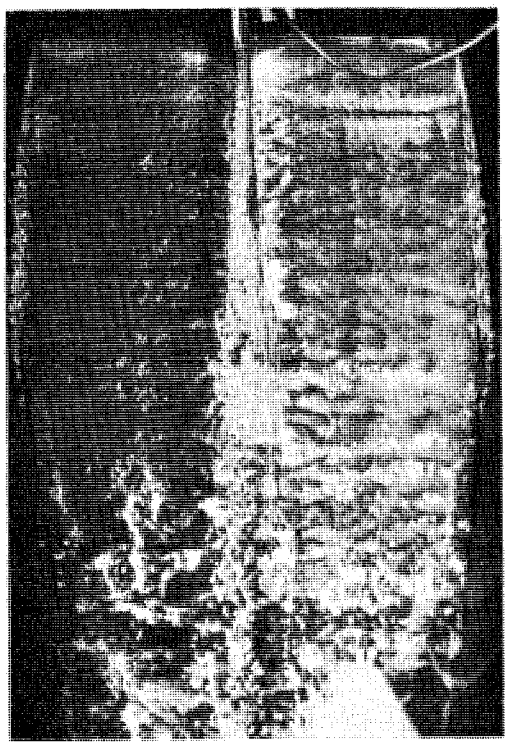

g. σ=.055 W= 14.09×10^{-3} lbs/sec.

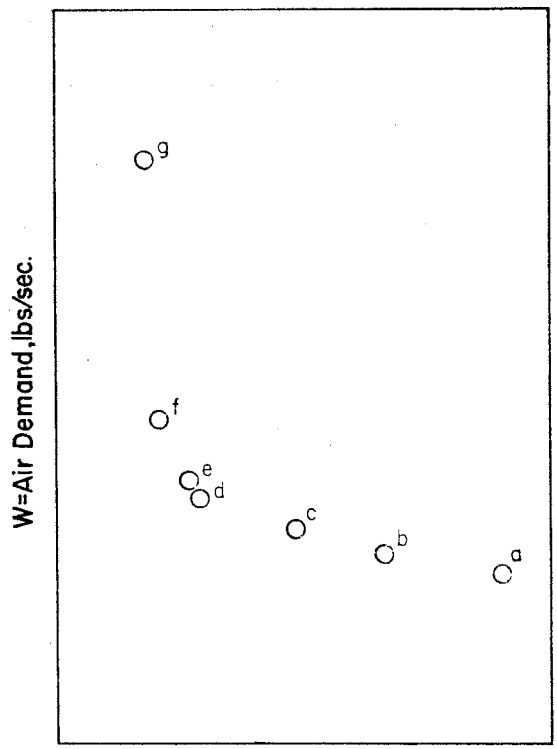

Fig. 13 cont.

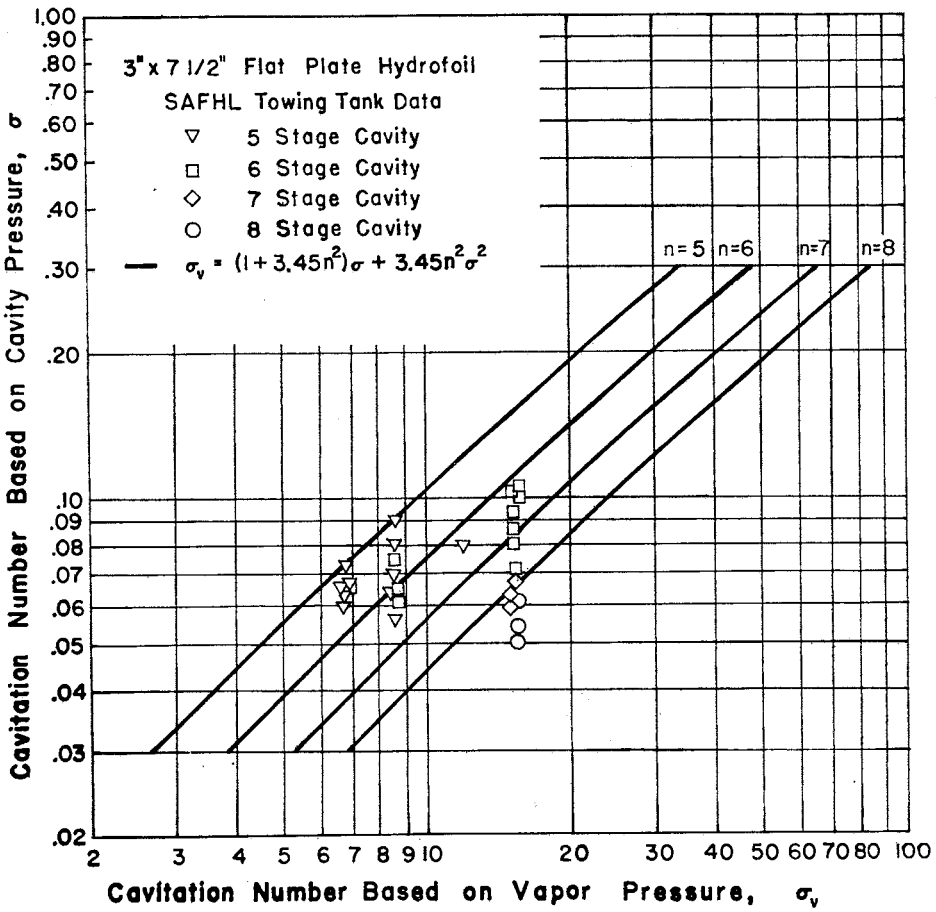

Fig. 14 - Comparison of Free-Jet Theory and Towing-Tank Data for Pulsating Cavities

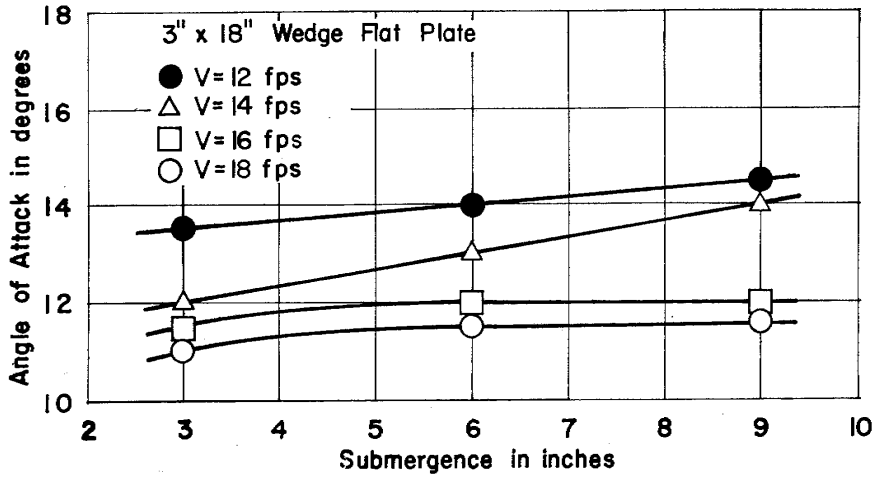

a. Effect of Submergence

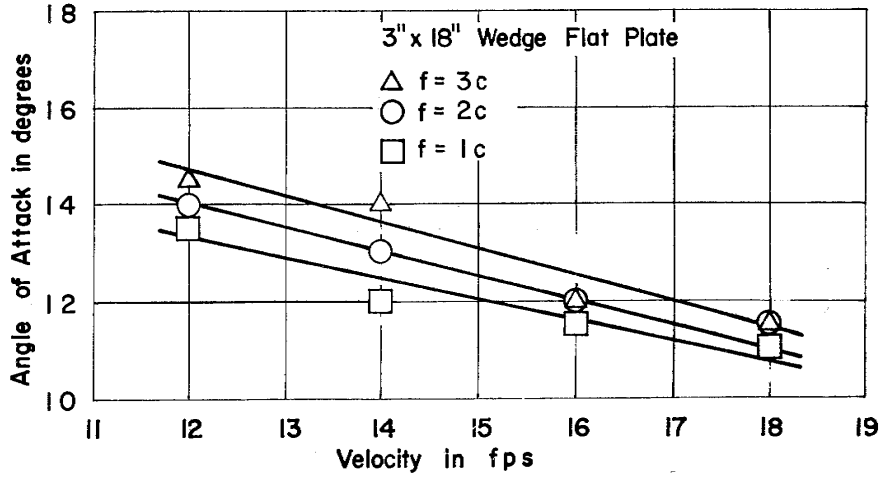

b. Effect of Velocity

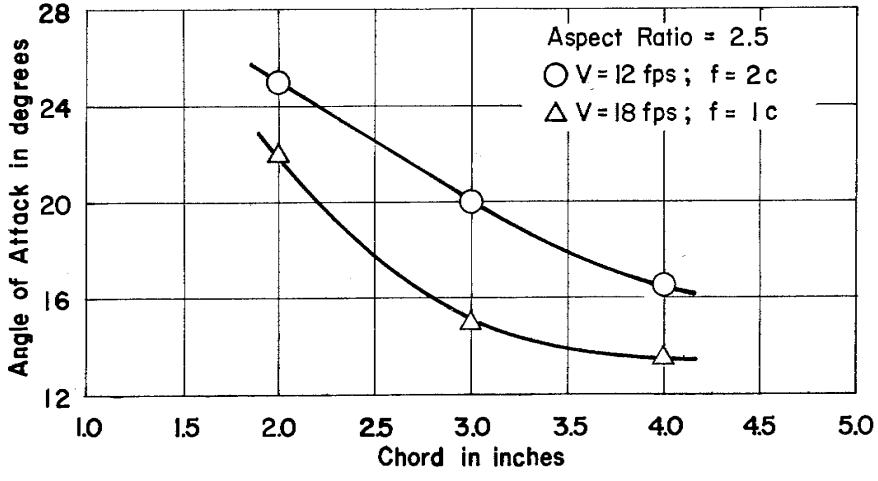

c. Effect of Chord

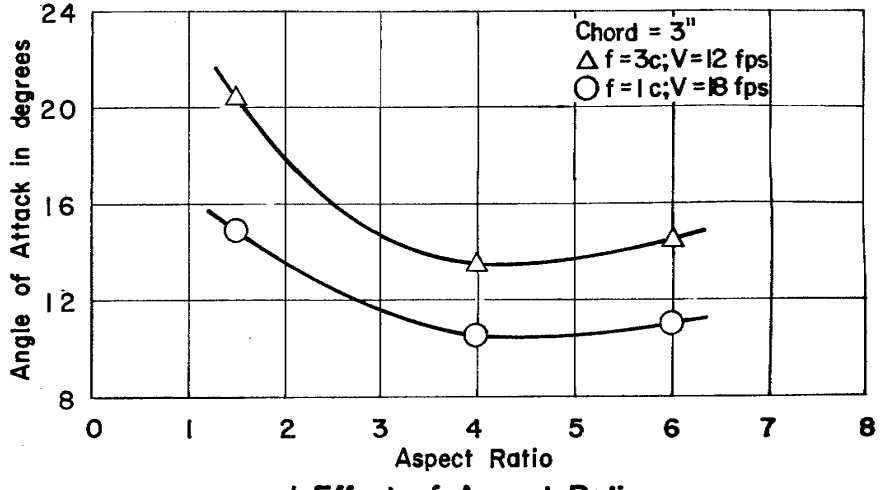

d. Effect of Aspect Ratio

Fig. 15 – Effect of Flow and Foil Parameters on Stability Threshold

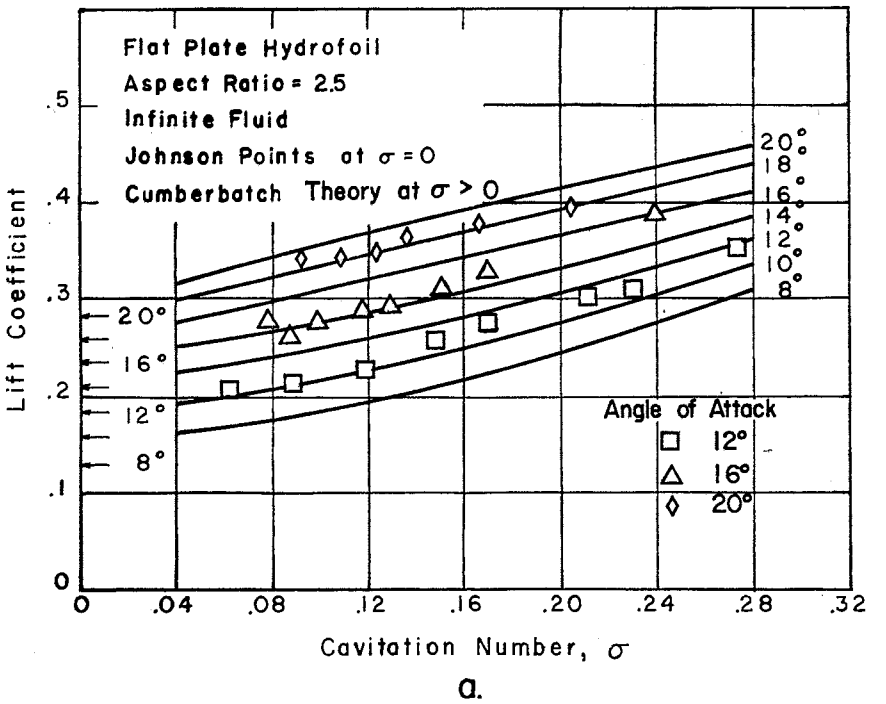

a.

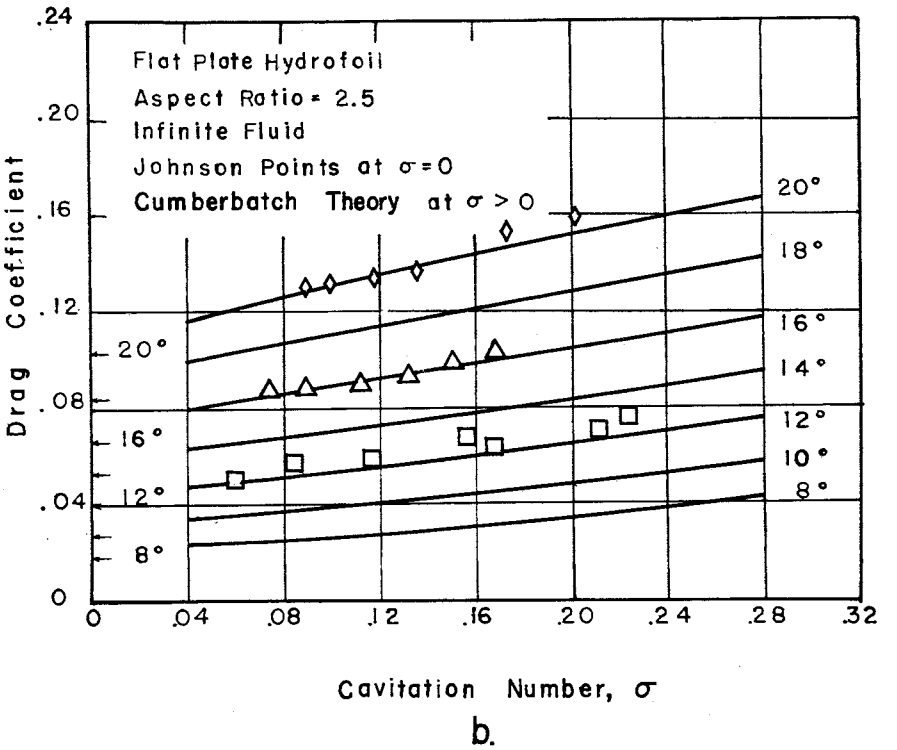

b.

Fig. 16 – Comparison of Theoretical and Experimental Force Coefficients.

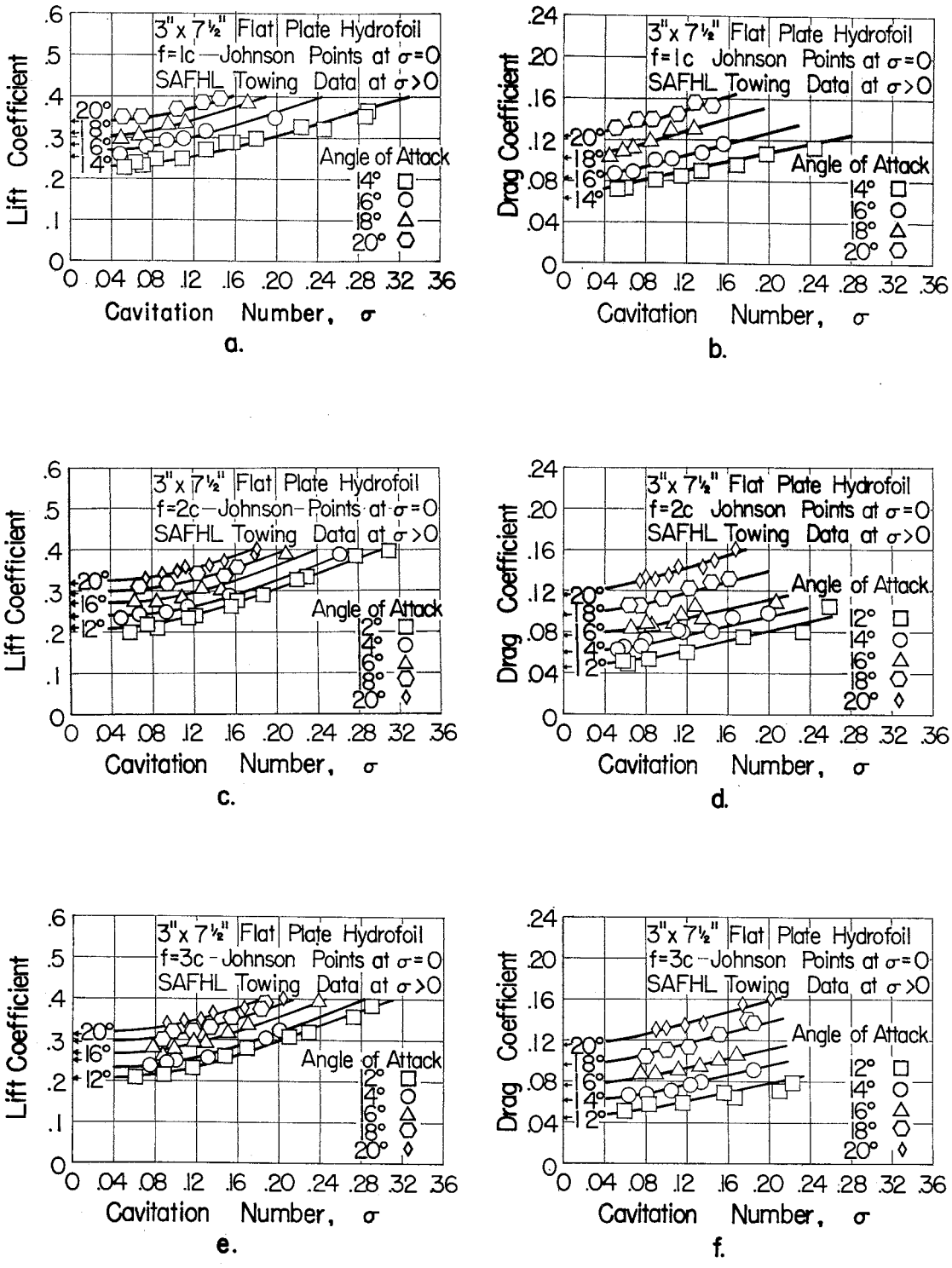

Fig. 17 - Force Coefficients for Flat Plate Foils, AR = 2.5

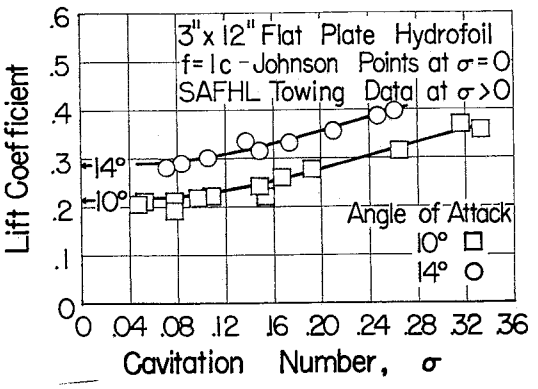

a.

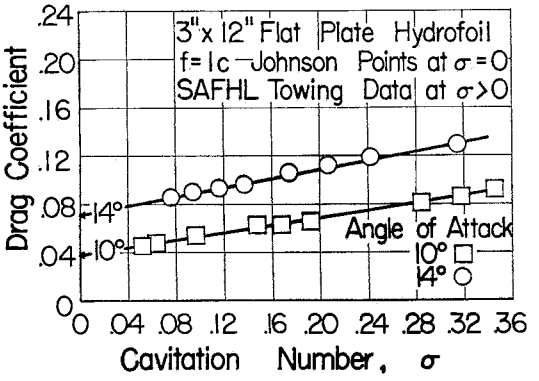

b.

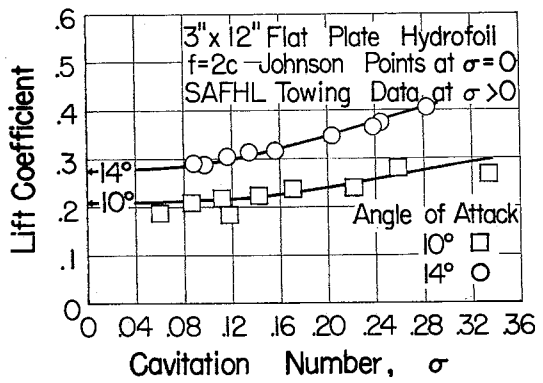

c.

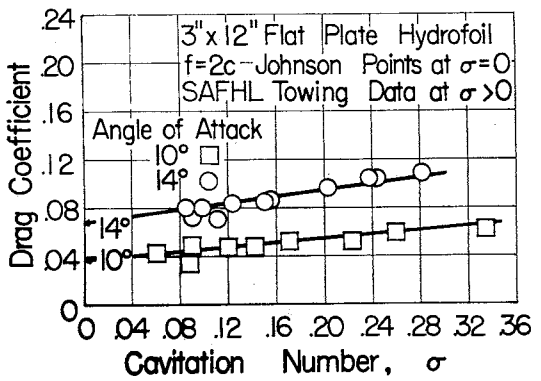

d.

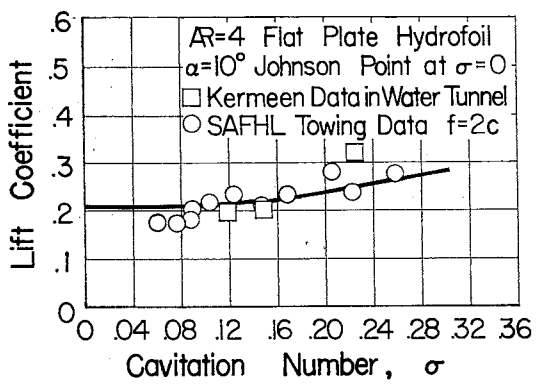

e.

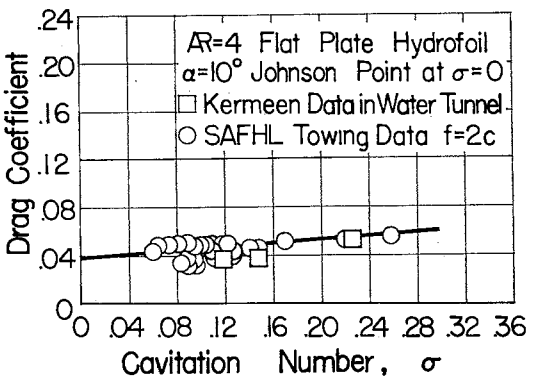

f.

Fig. 18 - Force Coefficients for Flat Plate Foils, AR = 4.0

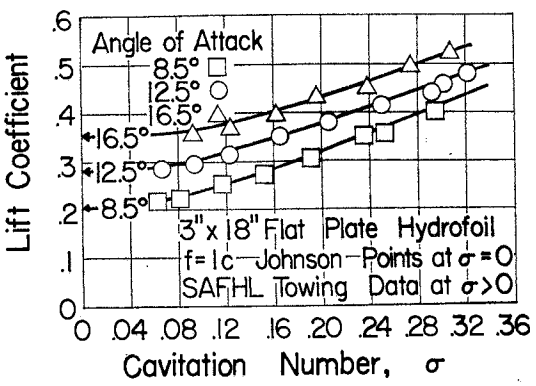

a.

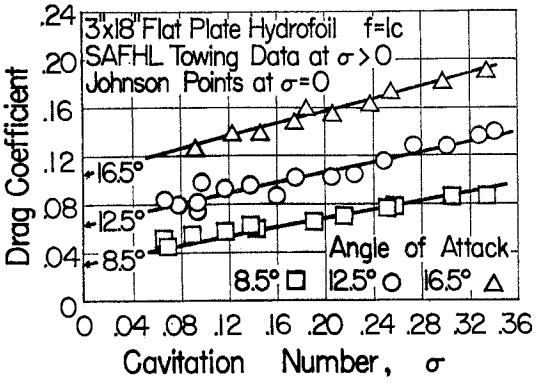

b.

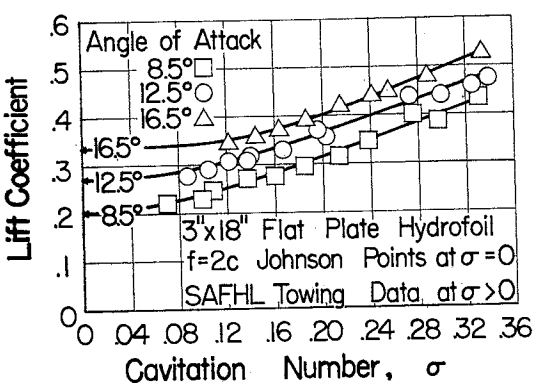

c.

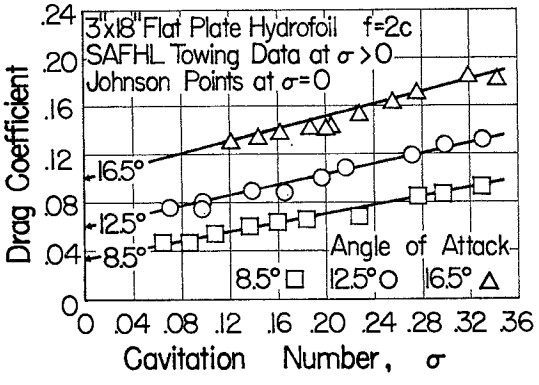

d.

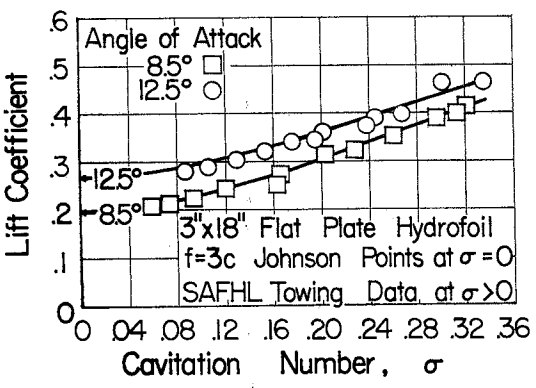

e.

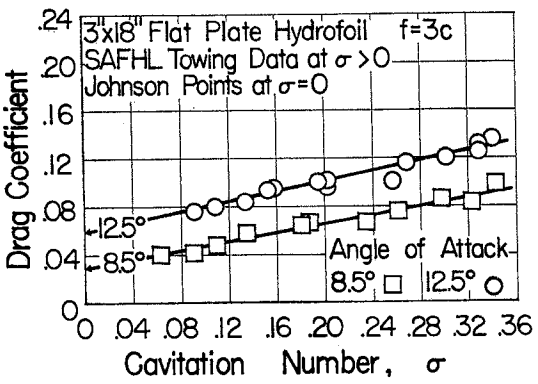

f.

Fig. 19 – Force Coefficients for Flat Plate Foils, AR = 6.0

SPONSOR'S DISTRIBUTION LIST FOR TECHNICAL PAPER NO. 36-B

of the St. Anthony Falls Hydraulic Laboratory

Copies	Organization
6	Chief of Naval Research, Department of the Navy, Washington 25, D. C., Attn: 3 - Code 438 1 - Code 461 1 - Code 463 1 - Code 466
1	Commanding Officer, Office of Naval Research Branch Office, 495 Summer Street, Boston 10, Massachusetts.
1	Commanding Officer, Office of Naval Research Branch Office, 346 Broadway, New York 13, New York.
1	Commanding Officer, Office of Naval Research Branch Office, 1030 East Green Street, Pasadena, California.
1	Commanding Officer, Office of Naval Research Branch Office, 1000 Geary Street, San Francisco 9, California.
25	Commanding Officer, Office of Naval Research Branch Office, Navy 100, Fleet Post Office, New York, New York.
6	Director, Naval Research Laboratory, Washington 25, D. C., Attn: Code 2027.
5	Chief, Bureau of Naval Weapons, Department of the Navy, Washington 25, D. C., Attn: 1 - Code RUAW-4 1 - Code RRRE 1 - Code RAAD 1 - Code RAAD-222 1 - Code DIS-42
8	Chief, Bureau of Ships, Department of the Navy, Washington 25, D. C., Attn: 1 - Code 310 1 - Code 312 1 - Code 335 1 - Code 420 1 - Code 421 1 - Code 440 1 - Code 442 1 - Code 449
1	Chief, Bureau of Yards and Docks, Department of the Navy, Washington 25, D. C., Attn: Code D-400.
15	Commanding Officer and Director, David Taylor Model Basin, Washington 7, D. C., Attn: 1 - Code 108 1 - Code 142

Copies	Organization
	1 - Code 500 1 - Code 513 1 - Code 520 1 - Code 526 1 - Code 526A 1 - Code 530 1 - Code 533 1 - Code 580 1 - Code 585 1 - Code 589 1 - Code 591 1 - Code 591A 1 - Code 700
1	Commander, U. S. Naval Ordnance Test Station, China Lake, California, Attn: Code 753.
1	Commander, U. S. Naval Ordnance Test Station, Pasadena Annex, 3202 E. Foothill Blvd., Pasadena 8, California, Attn: Code P-508.
1	Commander, Planning Department, Portsmouth Naval Shipyard, Portsmouth, New Hampshire.
1	Commander, Planning Department, Boston Naval Shipyard, Boston 29, Massachusetts.
1	Commander, Planning Department, Pearl Harbor Naval Shipyard, Navy 128, Fleet Post Office, San Francisco, California.
1	Commander, Planning Department, San Francisco Naval Shipyard, San Francisco 24, California.
1	Commander, Planning Department, Mare Island Naval Shipyard, Vallejo, California.
1	Commander, Planning Department, New York Naval Shipyard, Brooklyn 1, New York.
1	Commander, Planning Department, Puget Sound Naval Shipyard, Bremerton, Washington.
1	Commander, Planning Department, Philadelphia Naval Shipyard, U. S. Naval Base, Philadelphia 12, Pennsylvania.
1	Commander, Planning Department, Norfolk Naval Shipyard, Portsmouth, Virginia.
1	Commander, Planning Department, Charleston Naval Shipyard, U. S. Naval Base, Charleston, South Carolina.
1	Commander, Planning Department, Long Beach Naval Shipyard, Long Beach 2, California.

Copies	Organization
1	Commander, Planning Department, U. S. Naval Weapons Laboratory, Dahlgren, Virginia.
1	Commander, U. S. Naval Ordnance Laboratory, White Oak, Maryland.
1	Dr. A. V. Hershey, Computation and Exterior Ballistics Laboratory, U. S. Naval Weapons Laboratory, Dahlgren, Virginia.
1	Superintendent, U. S. Naval Academy, Annapolis, Maryland, Attn: Library.
1	Superintendent, U. S. Naval Postgraduate School, Monterey, California.
1	Commandant, U. S. Coast Guard, 1300 E Street, N. W., Washington, D. C.
1	Secretary Ship Structure Committee, U. S. Coast Guard Headquarters, 1300 E Street, N. W., Washington, D. C.
1	Commander, Military Sea Transportation Service, Department of the Navy, Washington 25, D. C.
3	U. S. Maritime Administration, GAO Building, 441 G Street, N. W., Washington, D. C., Attn: 1 - Division of Ship Design 1 - Division of Research 1 - Mr. R. P. Godwin
1	Superintendent, U. S. Merchant Marine Academy, Kings Point, Long Island, New York, Attn: Capt. L. S. McCready (Dept. of Engineering).
1	Commanding Officer and Director, U. S. Navy Mine Defense Laboratory, Panama City, Florida.
1	Commanding Officer, NROTC and Naval Administrative Unit, Massachusetts Institute of Technology, Cambridge 39, Massachusetts.
2	U. S. Army Transportation Research and Development Command, Fort Eustis, Virginia, Attn: Marine Transport Division.
1	Director of Research, National Aeronautics and Space Administration, 1512 H Street, N. W., Washington 25, D. C.
4	Director, Langley Research Center, Langley Field, Virginia, Attn: 2 - Mr. J. B. Parkinson 1 - Mr. I. E. Garrick 1 - Mr. D. J. Marten
1	Director Engineering Sciences Division, National Science Foundation, 1951 Constitution Avenue, N. W., Washington 25, D. C.

Copies	Organization
3	Director, National Bureau of Standards, Washington 25, D. C., Attn: 1 - Fluid Mechanics Division (Dr. G. B. Schubauer) 1 - Dr. G. H. Keulegan 1 - Dr. J. M. Franklin
10	Armed Services Technical Information Agency, Arlington Hall Station, Arlington 12, Virginia.
1	Office of Technical Services, Department of Commerce, Washington 25, D. C.
3	California Institute of Technology, Pasadena 4, California, Attn: 1 - Professor M. S. Plesset 1 - Professor T. Y. Wu 1 - Professor A. J. Acosta
1	University of California, Department of Engineering, Los Angeles 24, California, Attn: Dr. A. Powell.
1	Director, Scripps Institute of Oceanography, University of California, La Jolla, California.
1	Professor M. L. Albertson, Department of Civil Engineering, Colorado A and M College, Fort Collins, Colorado.
1	Professor J. E. Cermak, Department of Civil Engineering, Colorado State University, Fort Collins, Colorado.
1	Professor W. R. Sears, Graduate School of Aeronautical Engineering, Cornell University, Ithaca, New York.
2	State University of Iowa, Iowa Institute of Hydraulic Research, Iowa City, Iowa, Attn: 1 - Dr. H. Rouse 1 - Dr. L. Landweber
2	Harvard University, Cambridge 38, Massachusetts, Attn: 1 - Professor G. Birkhoff (Dept. of Mathematics) 1 - Professor G. F. Carrier (Dept. of Mathematics)
2	Massachusetts Institute of Technology, Cambridge 39, Massachusetts, Attn: 1 - Department of Naval Architecture and Marine Engineering 1 - Professor A. T. Ippen
3	University of Michigan, Ann Arbor, Michigan, Attn: 1 - Professor R. B. Couch (Dept. of Naval Architecture) 1 - Professor W. W. Willmarth (Aero. Engrg. Department) 1 - Professor M. S. Uberoi (Aero. Engrg. Department)
3	Dr. L. G. Straub, Director, St. Anthony Falls Hydraulic Laboratory, University of Minnesota, Minneapolis 14, Minnesota, Attn: 1 - Mr. J. M. Wetzel 1 - Mr. E. Silberman

Copies	Organization
1	Professor J. J. Foody, Engineering Department, New York State University Maritime College, Fort Schulyer, New York.
3	New York University, Institute of Mathematical Sciences, 25 Waverly Place, New York 3, New York, Attn: 1 - Professor J. Keller 1 - Professor J. J. Stoker 1 - Professor R. Kraichman
3	The Johns Hopkins University, Department of Mechanical Engineering, Baltimore 18, Maryland, Attn: 1 - Professor S. Corrsin 2 - Professor O. M. Phillips
1	Massachusetts Institute of Technology, Department of Naval Architecture and Marine Engineering, Cambridge 39, Massachusetts, Attn: Prof. M. A. Abkowitz, Head.
2	Dr. G. F. Wislicenus, Ordnance Research Laboratory, Pennsylvania State University, University Park, Pennsylvania, Attn: Dr. M. Sevik.
1	Professor R. C. DiPrima, Department of Mathematics, Rensselaer Polytechnic Institute, Troy, New York.
5	Stevens Institute of Technology, Davidson Laboratory, Castle Point Station, Hoboken, New Jersey, Attn: 1 - Professor E. V. Lewis 1 - Mr. D. Savitsky 1 - Mr. J. P. Breslin 1 - Mr. C. J. Henry 1 - Mr. S. Tsakonas
1	Webb Institute of Naval Architecture, Crescent Beach Road, Glen Cove, New York, Attn: Technical Library.
1	Director, Woods Hole Oceanographic Institute, Woods Hole, Massachusetts.
1	Executive Director, Air Force Office of Scientific Research, Washington 25, D. C., Attn: Mechanics Branch.
1	Commander, Wright Air Development Division, Aircraft Laboratory, Wright-Patterson Air Force Base, Ohio, Attn: Mr. W. Mykytow, Dynamics Branch.
2	Cornell Aeronautical Laboratory, 4455 Genesee Street, Buffalo, New York, Attn: 1 - Mr. W. Targoff 1 - Mr. R. White
3	Massachusetts Institute of Technology, Fluid Dynamics Research Laboratory, Cambridge 39, Massachusetts, Attn: 1 - Professor H. Ashley 1 - Professor M. Landahl 1 - Professor J. Dugundji

Copies	Organization
2	Hamburgische Schiffbau-Versuchsanstalt, Bramfelder Strasse 164, Hamburg 33, Germany, Attn: 1 - Dr. O. Grim 1 - Dr. H. W. Lerbs
1	Institut für Schiffbau der Universität Hamburg, Berliner Tor 21, Hamburg 1, Germany, Attn: Professor G. P. Weinblum, Director.
1	Max-Planck Institut für Stromungsforschung, Bottingerstrasse 6/8, Gottingen, Germany, Attn: Dr. H. Reichardt.
1	Hydro-og Aerodynamisk Laboratorium, Lyngby, Denmark, Attn: Professor Carl Prohaska.
1	Skipsmodelltanken, Trondheim, Norway, Attn: Professor J. K. Lunde.
1	Versuchsanstalt für Wasserbau und Schiffbau, Schleuseninsel im Tiergarten, Berlin, Germany, Attn: Dr. S. Schuster, Director.
1	Technische Hogeschool, Institut voor Toegepaste Wiskunde, Julianalaan 132, Delft, Netherlands, Attn: Professor R. Timman.
1	Bureau D'Analyse et de Recherche Appliquees, 47 Avenue Victor Cresson, Paris 8, France, Attn: Professor L. Malavard.
1	Netherlands Ship Model Basin, Wageningen, Netherlands, Attn: Dr. Ir. J. D. van Manen.
1	Allied Research Associates, Inc., 43 Leon Street, Boston 15, Massachusetts, Attn: Dr. T. R. Goodman.
3	National Physical Laboratory, Teddington, Middlesex, England, Attn: 1 - Dr. F. H. Todd, Superintendent Ship Division 1 - Head Aerodynamics Division 1 - Mr. A. Silverleaf
2	Head, Aerodynamics Department, Royal Aircraft Establishment, Farnborough, Hants, England, Attn: Mr. M. O. W. Wolfe.
1	Boeing Airplane Company, Seattle Division, Seattle, Washington, Attn: Mr. M. J. Turner.
1	Electric Boat Division, General Dynamics Corporation, Groton, Connecticut, Attn: Mr. Robert McCandliss.
1	General Applied Sciences Labs, Inc., Merrick and Stewart Avenues, Wesbury, Long Island, New York.
1	Gibbs and Cox, Inc., 21 West Street, New York, New York.
3	Grumman Aircraft Engineering Corp., Bethpage, Long Island, New York, Attn: 1 - Mr. E. Baird 1 - Mr. E. Bower 1 - Mr. W. P. Carl

Copies	Organization
1	Lockheed Aircraft Corporation, Missiles and Space Division, Palo Alto, California, Attn: R. W. Kermeen.
1	Midwest Research Institute, 425 Volker Blvd., Kansas City 10, Missouri, Attn: Mr. Zeydel.
3	Director, Department of Mechanical Sciences, Southwest Research Institute, 8500 Culebra Road, San Antonio 6, Texas, Attn: 1 - Dr. H. N. Abramson 1 - Mr. G. Ransleben 1 - Editor, Applied Mechanics Reviews
3	Convair, A Division of General Dynamics, San Diego, California, Attn: 1 - Mr. R. H. Oversmith 1 - Mr. A. D. MacLellan 1 - Mr. H. T. Brooke
1	Dr. S. F. Hoerner, 148 Busteed Drive, Midland Park, New Jersey.
1	Hydronautics, Incorporated, 200 Monroe Street, Rockville, Maryland. Attn: Mr. Phillip Eisenberg.
1	Rand Development Corporation, 13600 Deise Avenue, Cleveland 10, Ohio, Attn: Dr. A. S. Iberall.
1	U. S. Rubber Company, Research and Development Department, Wayne, New Jersey, Attn: Mr. L. M. White.
1	Technical Research Group, Inc., 2 Aerial Way, Syosset, Long Island, New York, Attn: Mr. Jack Kotik.
1	Mr. C. Wigley, Flat 102, 6-9 Charterhouse Square, London, E. C. 1, England.
1	AVCO Corporation, Lycoming Division, 1701 K Street, N. W., Apt. No. 904, Washington, D. C., Attn: Mr. T. A. Duncan.
1	Mr. J. G. Baker, Baker Manufacturing Company, Evansville, Wisconsin.
1	Curtiss-Wright Corporation Research Division, Turbomachinery Division, Quehanna, Pennsylvania, Attn: Mr. George H. Pedersen.
1	Hughes Tool Company, Aircraft Division, Culver City, California, Attn: Mr. M. S. Harned.
1	Lockheed Aircraft Corporation, California Division, Hydrodynamics Research, Burbank, California, Attn: Mr. Bill East.
1	National Research Council, Montreal Road, Ottawa 2, Canada, Attn: Mr. E. S. Turner.

Copies	Organization
1	The Rand Corporation, 1700 Main Street, Santa Monica, California, Attn: Technical Library.
2	Stanford University, Department of Civil Engineering, Stanford, California, Attn: 1 - Dr. Byrne Perry 1 - Dr. E. Y. Hsu
1	Waste King Corporation, 5550 Harbor Street, Los Angeles 22, California, Attn: Dr. A. Schneider.
1	Mr. David Wellinger, Hydrofoil Projects, Radio Corporation of America, Burlington, Massachusetts.
2	Versuchsanstalt fur Wasserbau und Schiffbau, Schleuseninsel im Tiergarten, Berlin, Germany, Attn: 1 - Dr. Grosse 1 - Dr. H. Schwanecke
1	Commanding Officer and Director, David Taylor Model Basin, Washington 7, D. C., Attn: Code 586.
1	Hydrofoil Corporation of America, P. O. Box 11055, San Diego 11, California, Attn: Mr. John Bader, President.
1	Dr. Hirsch Cohen, IBM Research Center, P. O. Box 218, Yorktown Heights, New York.
1	Food Machinery Corporation, P. O. Box 367, San Jose, California, Attn: Mr. G. Tedrew.
1	Dr. Blaine R. Parkin, Air Research Manufacturing Corp., 9851-9951 Sepulveda Boulevard, Los Angeles 45, California.